FACULDADE DE ENGENHARIA DA UNIVERSIDADE
DO PORTO

Sound Wave Phase Processing for Precise Positioning

Diana Catarino das Neves Viegas

Mestrado em Métodos Computacionais em Ciências e Engenharia

December 2005

Advisor: Sérgio Reis Cunha

Discovery consists in seeing what everyone else has seen and thinking what no one else has thought.

Albert Szent-Gyorgi, 1937 Nobel Prize in Physiology and Medicine

Resumo

Actualmente, os sistemas de navegação por satélite alcançaram um nível de maturidade elevado, atingindo presentemente precisões centimétricas. Dentro deste tipo de sistemas, destaca-se com supremacia o sistema GPS (Global Positioning System), tendo sido um dos principais marcos dos sistemas de posicionamento nos últimos 10 anos. Contudo, estes sistemas não são eficientes em ambientes fechados uma vez que a potência e a gama de frequências utilizadas não permitem a penetração desta radiação através de paredes, tornando praticamente impossível a localização dentro de edifícios. O recursos a sinais de oportunidade, ou seja, sinais que existem para outros fins que não a localização, permite o posicionamento dentro de edifícios uma vez que as frequências utilizadas neste tipo de sinais estão em gamas que penetram paredes. São exemplo as estações emissoras de rádio e televisão, no entanto, é necessário desenvolver novas aproximações aos algoritmos de posicionamento existentes de modo a alcançar uma precisão centimétrica na localização de um receptor, no sentido em que os sinais de oportunidade não transportam qualquer tipo de informação que possa ser utilizada como referência para localização.

Este trabalho pretende ser uma prova de que é possível desenvolver algoritmos de posicionamento baseados em medições de fase de diversos sinais sinusoidais puros, envolvendo métodos de resolução de ambiguidades. Os resultados obtidos são suportados por ensaios utilizando sinais acústicos, com comprimentos de onda da mesma ordem de grandeza que os que seriam utilizados em rádio frequência, com a finalidade de localização com precisão centimétrica. Por outro lado, a utilização de sinais acústicos torna-se igualmente interessante, uma vez que os sinais acústicos podem ser de extrema importância em determinados ambientes.

Abstract

Outdoor navigation has evolved to a high degree of maturity and precision due mainly to satellite based systems, where GPS has played a major role in the past 10 years. Compact and self-contained navigation instruments became a reality in a wide range of different applications, some of them achieving centimetre-level accuracy. However, satellite based systems are not effective in indoor environment, since the transmitted electromagnetic waves use frequencies and power levels that do not penetrate into buildings. The use of signals of opportunity, which are existing radio waves that are transmitted for other reasons than radiolocation, like radio and TV broadcast stations, is an emerging way to compute a receiver position with centimetric accuracy in indoor environment. Since the transmitted signals do not carry any information that can be used as reference for ranging, different algorithmic approaches have to be developed for this purpose.

This dissertation is a proof-of-concept study on positioning algorithms based on differential ranging between a pair of receivers using only phase measurements of multiple single frequency waves, involving integer ambiguity resolution methods. This work and its results are supported by experiments using audio signals with wavelengths of the same order of magnitude of the radio waves that would be suitable for indoor radiolocation. Besides enabling such study with a more friendly hardware setup, acoustic signals are by themselves useful in specific navigation environments.

Acknowledgements

Many people have contributed, directly or indirectly, to this thesis. To all of them, and especially to those I am about to mention, I would like to convey my heartfelt thanks.

First of all, I would like to thank my teacher, Sérgio Reis Cunha, who gave me the opportunity to work with positioning systems. His trust and willingness to supervise me have instilled in me an uncomprising sense of perseverance in moments of greater doubt. I am indebted to him for the patience when trying to understand my difficulties and, above all, for the valuable teachings and exemplar scientific counselling.

Secondly, I would like to convey my thanks to Professor Francisco Restivo, as responsible for the Institute for Development and Technological Innovation (Instituto de Desenvolvimento e Inovação Tecnológica - IDIT), for the means he made available, especially for the anechoic chamber without which this work would not be possible.

I would also like to acknowledge the support of Sérgio Rui Silva, without which this work would not be possible. I thank him for the friendly words and, most of all, the teachings and suggestions of priceless scientific value.

I must also thank my friends, especially Sandra Paiva and Hugo Silva, for their understanding of my absence this last year and for the support they have given me regardless of everything.

A final word to my family, for the unrelenting support and understanding despite the little time I have been able to spend with them.

Contents

List of Figures

List of Tables

Chapter 1

Introduction

Summary: *Nowadays positioning systems are well known and frequently used. Outdoor navigation systems, satellite navigation and, in particular, GPS, has reached a very mature state for outdoor navigation. However, present-day needs have lead to a demand for accurate indoor location, which has not been achieved yet. Actual indoor positioning systems are not effective and have not a high accuracy level. As an introduction, this chapter presents a brief description of the work, explaining the motivation, the target objectives and several relevant scientific contents employed.*

1.1 Motivation

Outdoor navigation systems are well known in a wide range of different applications. Satellite based systems are, undoubtedly, one of the bests applications, where Global Positioning System (GPS) has played the major role. Personal navigation systems have developed tremendously, reaching now the frontier of positioning inside buildings. It has become relevant to track the location of a person or a specific object inside buildings, such as malls or museums, or even tracking assets in warehouses.

Despite the vast number of applications and the high precision of satellite based systems, they are not effective in indoor environment or in dense urban areas due to its weak signal reception when there are no lines-of-sight from a mobile station to, at least, three GPS satellites [DR01]. The transmitted electromagnetic waves use frequencies and power levels that barely penetrate into buildings. As a result, indoor positioning systems require alternative means to detect the location of the mobile station. Radiofrequency signals from radio and TV broadcast stations are in a bandwidth that is more friendly for this type of applications [Hal02]. So, the use of signals of opportunity is an emerging way to detect and track a receiver with centimetric accuracy in indoor environment, because there is no need for bandwidth reservation. This solution may present itself as most advantageous both commercial and market-wise, mostly because no further frequency licensing would be asked for, since previously licensed frequencies would be used from opportunity signals. The simplicity of this concept might improve indoor positioning systems.

1.2 State-of-the-art

The success of outdoor positioning and satellite based applications provides an incentive for the research and development of indoor positioning systems.

Ultrasound, infrared and radiofrequency (RF) signals are the major sensing technologies used for the indoor environment. Some researchers have been successful, to a limited extent, in developing GPS based indoor location systems by using high-sensitivity receivers [DA01]. Since higher sensitivity is achieved through higher correlation times between sensed and reference signals, position accuracy is severely degraded. Besides all the attempts done in GPS based indoor location systems and its high-sensitivity receivers, these systems have a moderate penetration into buildings, due to its signals wavelength. So, the GPS based indoor location systems are limited to its signals penetration restrictions. Others have used a combination of radiofrequencies and ultrasound [HHS+99] or infrared signal [WHFG92] for indoor positioning. All these location systems have their own strengths and are very useful in their respective application domains.

SpotOn [HBW02] and *RADAR* [BP00] are two significant of the many RF based indoor positioning systems that use RF signal, such as wireless LAN and Bluetooth, to locate indoor objects. These systems measure distance between transmitter and receiver based on received signal strength information (RSSI) of the RF signals, and compute location of object from information only. However, it is difficult to measure precise distance using the received signal strength and the estimated position accuracy is not better than a few meters. Of course, it is possible to utilize ultra wide band (UWB) technology [Cyg04] to measure precise range based on time-difference-of-arrival (TDOA), but it usually requires complex hardware.

Active Bat [HHS+99] and *Cricket location-support system* [PCB99] are systems that use ultrasonic pulse TDOA to enable high precision 3-dimensional positioning in indoor environment. Although ultrasonic positioning system requires additional hardware to send and receive ultrasonic pulse, it can determine 3D position of indoor objects with accuracy between a few millimetres and a few centimetres. However, both RF-based and ultrasonic-based systems usually require many manual pre-configuration of the locations of reference stations in

order to determine precise object positions.

These pioneer works in this area have some disadvantages, such as the limitation of the infrared or ultrasound sensing signals which cannot penetrate into walls and floors. Most of these systems need the use of specialized hardware which is not easily available. Also, some of these systems are prohibitively expensive for wide deployment.

The use of signals of opportunity has been explored for positioning only to mild extent. Since these signals are not structured for positioning, the position computation techniques can only rely very simple characteristics of the received waves, such as amplitude and phase. The latter is far for more precise, although more difficult to process. This is the approach followed in this dissertation. Other similar approaches can be found in [Hal02] where relative position between a based station, in a known fixed position, and a rover station is determined by multilateration from observations of the carrier phase of signals received from AM broadcast stations.

Several methods were developed to determine positions by carrier phase observations [Hab99], [DR01]. The Global Navigation Satellite System (GLONASS) is an example of the use of different frequencies for positioning through phase processing. A GLONASS receiver can separate the signal of a particular satellite from the total incoming signal of all visible satellites by assigning different frequencies to its tracking channels. This technique is called Frequency Division Multiple Access (FDMA). With FDMA there is no need to distinguish satellites by signal modulation, which is different to the technique used for signals transmitted by GPS satellites. Each GPS satellite modulates similar carrier frequencies with a different code, a procedure that is called Code Division Multiple Access (CDMA). Therefore there is no need for different frequencies in GPS, and all GPS satellites use the same frequencies [Hab99]. Regarding carrier phase positioning methods, the main difference between GLONASS and GPS systems rises from the use of several frequencies in GLONASS, compared to the use of only

one (or two) frequencies in the GPS case. Phase coherence analysis of GLONASS is similar to those of GPS except for the satellite-specific GLONASS frequencies. However, a new bias term remains in a double difference phase combination for GLONASS. Its magnitude depends on the wavelength difference of the two satellites and is not present in case of GPS.

Ambiguity resolution methods or integer parameter estimation became one of the most important issues in navigation based on phase measurements. The LAMBDA method for GPS ambiguity resolution is widely employed to facilitate the search for correct integer solutions [HB98], [dTT96]. However, for the case of several frequencies, like the GLONASS system, further terms have to be estimated during ambiguity resolution [Hab99].

1.3 Target Objectives

This dissertation is an initial study of location algorithms for indoor positioning systems based on phase processing of opportunity signals. As opportunity signals do not carry any information that can be used as reference for positioning, like satellite based systems do, different algorithmic approaches have to be developed for this purpose.

This work intends to be a *proof-of-concept* study on positioning algorithms. The location is based on differential ranging between a pair of receivers using only phase measurements of multiple acoustic single phase frequencies. In order to depend on nothing else than opportunity signals, only sinusoids were used.

As mentioned before, the results obtained were supported by experiments using audio signals with wavelengths of the same order of magnitude of the radio waves that would be suitable for indoor radiolocation. This choice is related to the simplicity of the hardware setup required to use acoustic waves and because acoustic signals are by themselves useful in specific navigation environments (e.g. underwater navigation).

The experimental setup used was composed of loud speakers as transmitters and microphones as receivers: ten transmitters (loud speakers), each of them transmitting a single frequency, and two receivers (microphones). One is placed in a known fixed position (reference receiver) and the other, potentially mobile, in unknown positions (roving receiver). The position of the rover is determined from comparison between the phase signals as captured by the roving and the reference receiver. The related algorithms involve integer parameter estimation to compute the position of the receiver.

1.4 Scientific Contents

Several different scientific topics were explored throughout this work. One of them is signal processing for real-time recovery of the phase of a received set of waves using FIR filters. Another topic is the developed mathematical model, similar to that of GLONASS [Hab99], to relate distance/position to phase measurements.

The main subject is the formulation and the solution of the position determination objective as a n-dimensional integer optimization problem. Figure 1.1 shows wavefront lines on which phase are constant for two transmitters producing different single frequency signals in a bi-dimensional space. The feasible solutions of rover positioning with signals from two transmitters correspond exactly to the intersection of the wavefronts from the two transmitters. Many solutions are admissible for only two transmitters, as shown. If there are three transmitter as illustrated on figure 1.2, the number of possible combinations increases. Every combination of wavefronts from three transmitters is possible. In spite of the increase of the admissible solutions, the feasible set for a problem with three transmitters decrease significantly. The feasible solutions, in this particular case, are only the solutions whose wavefront intersects in the same point. This solutions are marked in figure 1.2 with a circle. For each transmitter added to the

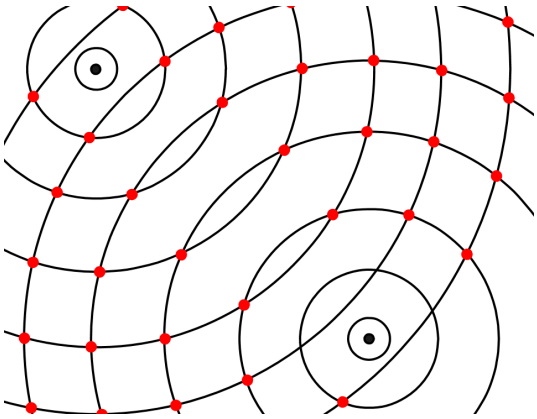

Figure 1.1 — Feasible solutions for two transmitters.

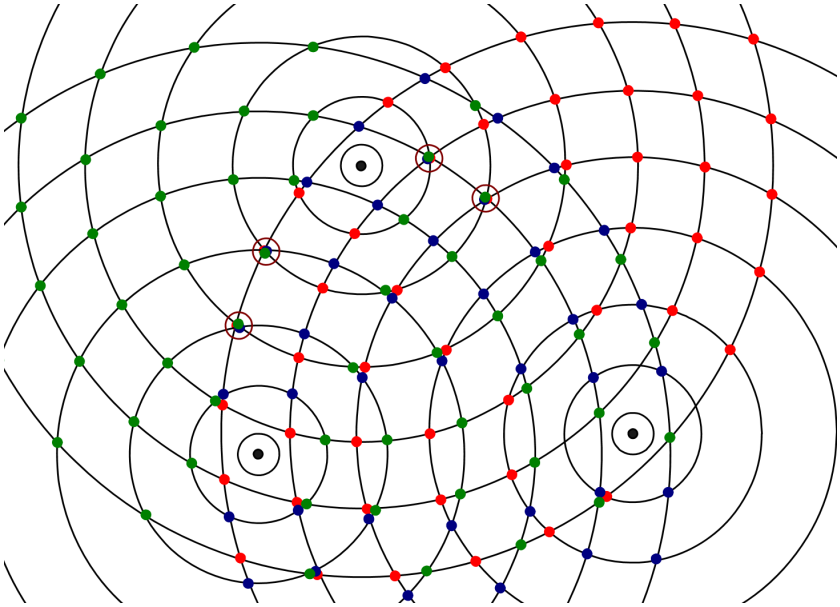

Figure 1.2 — Feasible solutions for three transmitters.

system, the admissible solutions will increase and the feasible solutions will reduce further. This is, obviously, a n-dimensional integer optimization problem, where n is the number of transmitters on the system. These figures shows only a problem with two coordinates, however the problem to solve in this dissertation has the third coordinate and time variables which cause a more complex problem to determine.

This n-dimensional problem can be expressed as a weighted least squares minimization problem with real and integer variables. The real variable depends

on the rover location and the integer variable depends on an integer number of wavelengths. This minimization is converted into two least-squares sub-problems: one is purely real and the other is a purely integer least-squares minimization. The last one is the challenge that this work addresses. Its solution involves a change of base on z maintaining an isomorphism from $\mathbb{Z}^q$ onto $\mathbb{Z}^q$. The probabilistic analysis of the residues to sort out the possible solutions is, also, an important aspect discussed in this dissertation.

1.5 Dissertation Layout

Chapter 2 explain some important physical concepts that will be useful in this work. Chapter 3 describes several issues about the employed hardware and the pre-processing used to compute phase measurements from the acquired data. Chapter 4 presents the mathematics and algorithmics of integer parameter estimation and ambiguity resolution. The description of the developed algorithms follows in chapter 5. Chapter 6 shows and discusses the experimental results and chapter 7 is devoted to conclusions and points towards future research activities.

Chapter 2

Sound Wave Propagation

Summary: *This chapter contains a simple explanation of physics related to sound wave propagation.*

Acoustics may be defined as the generation, transmition and reception of energy in the form of vibracional waves in matter. As atoms or molecules of a fluid or a solid are displaced from their normal configurations, an internal elastic restoring force arises.

2.1 Wave Equation

The acoustic quantities are related to the fundamental laws of physics, which are:

- Newton´s law governs the motion of particles, stated in 2.1

$$\nabla p = -\rho \frac{dv}{dt} \tag{2.1}$$

  where p is the instantaneous fluid local pressure, ρ is the mass density and v the velocity of the particle.

- The particles mass is constant (principle of conservation of the mass).

- A compressibility law governs the particles deformation.

The sound wave equation is obtained applying these laws to a particle, combining and linearizing them. Although each physical process has specific laws of dynamics, there is an equation for all kinds of ondulatory motions, since Newton´s law governs the motion of particles.

The most general case is the propagation of sound waves in the three dimensional space. The wave equation for pressure is deduced from Newton´s law taking under the hypothesis of small motions [KFCS82]. This equation is expressed in 2.2

$$\nabla^2 p - \left(\frac{\rho}{K}\right) \frac{d^2 p}{dt^2} = 0 \tag{2.2}$$

where p is the pressure, ρ is the mass density in Kg/m^3 and K is the bulk modulus of the fluid, expressed in Pa. The dimensional analysis of 2.2 shows that the ratio

$\frac{K}{\rho}$ has the dimension of a squared speed. So, the speed of sound can be defined as

$$c = \left(\frac{\rho}{K}\right)^{\frac{1}{2}}$$

and the wave equation can be transformed into

$$\nabla^2 p - \frac{1}{c^2}\frac{d^2 p}{dt^2} = 0 \tag{2.3}$$

This equation is called d'Alembert equation and governs the phenomena of lossless linear propagation. It characterizes wave propagation in many other fields as, for example, electromagnetic.

Taking the parallelism between acoustic and electromagnetic waves application into account for this kind of work, the wave equations for both cases are similar. The reason are not related to in the phenomena themselves, which are completely different in nature, but in their models. Thus, it is the closeness of the models conveying a similar behaviour that sustains the use of acoustic waves as a proof-of-concept for future radio wave based indoor navigation systems.

Maxwell´s equations constitute the most complete formulation of the interactions of electromagnetic quantities [LCL00]. The electromagnetic wave equation for one dimension is obtained deriving the Maxwell´s equations and is expressed as,

$$\frac{d^2 a}{dx^2} - \frac{1}{c^2}\frac{d^2 a}{dt^2} = 0 \tag{2.4}$$

where c is the speed of light, $a = A\cos(wt \pm kx)$ and w is the angular speed. $k = \frac{2\pi}{\lambda}$ is the wave number where λ is the wavelength. For a generic case of a three dimensional situation the wave equation is stated as,

$$\nabla^2 a - \frac{1}{c^2}\frac{d^2 a}{dt^2} = 0 \tag{2.5}$$

This equation is similar to 2.3; however the variables have different physical meanings.

2.2 Radiation from a Plane Circular Piston

In order to understand the behaviour of the sound sources used in this work, as a first approximation, it is considered that real sources have the same properties as the theoretical ones. The behaviour of the loudspeakers can be compared to the theoretical model of a circular piston mounted in an infinite baffle and vibrating with simple harmonic motion as shown in figure 2.1.

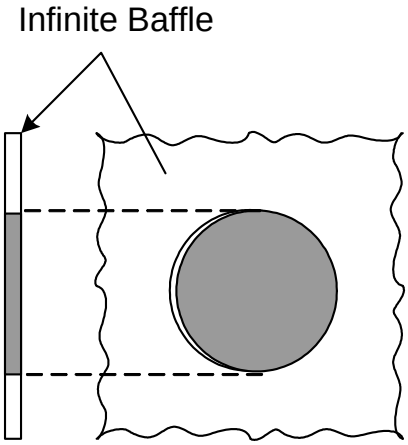

Figure 2.1 — Schematic view of a circular piston in an infinite baffle.

The circular piston is considered a flat, thin and rigid disk of radius a, driven by a sinusoidal oscillating translatory movement along its axis of uniform velocity $U_0 exp\,(jwt)$. The radiated sound field has symmetry of revolution with the same axis as the piston. The geometry and coordinates are sketched in figure 2.2.

2.2.1 Far and Near Field Definitions

The radiated sound pressure is obtained by summing the contribution of each element dS, i.e. by integrating over the surface of the piston. The total pressure generated is given by [KFCS82]

$$p(r,\theta,t) = j\frac{\rho c U_0 k}{2\pi}\int_S \frac{e^{j(wt-kr')}}{r'}dS \tag{2.6}$$

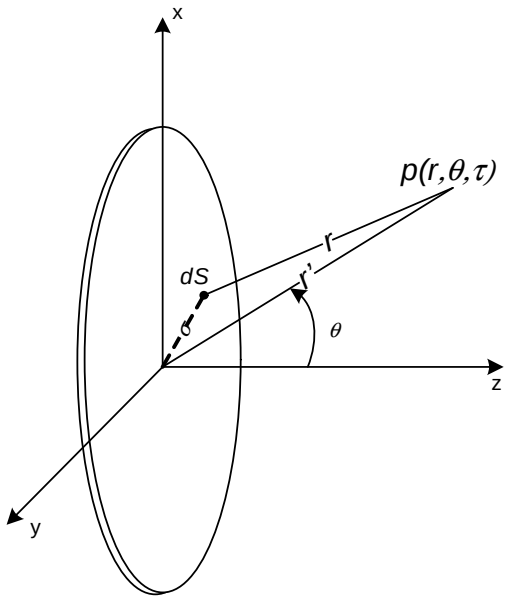

Figure 2.2 — Geometry used in deriving the radiation characteristics of a flat piston.

where c is the sound speed, k is the wave number and the surface integral is taken over the region $\sigma \leq a$. The field along the acoustic axis (the z axis) is relatively simple to calculate. With reference to figure 2.2 the pressure is,

$$p(r,0,t) = j\frac{\rho c U_0 k}{2\pi} e^{jwt} \int_0^a \frac{exp\left(-jk\sqrt{r^2+\sigma^2}\right)}{\sqrt{r^2+\sigma^2}} 2\pi\sigma d\sigma \tag{2.7}$$

After mathematical manipulations [KFCS82], the pressure amplitude on the axis of the piston is the magnitude of the expression 2.8,

$$p(r,0) = 2\rho c U_0 \left| \sin\left\{ \frac{1}{2} kr \left[\sqrt{1+\left(\frac{a}{r}\right)^2} - 1 \right] \right\} \right| \tag{2.8}$$

For $\frac{r}{a} \gg 1$, the square root can be simplify to

$$\sqrt{1+\left(\frac{a}{r}\right)^2} = 1 + \frac{1}{2}\left(\frac{a}{r}\right)^2$$

If also $\frac{r}{a} \gg ka$, the field point is distant compared to both the radius and wavelength, then the pressure amplitude on axis has asymptotic form as shown in expression 2.9

$$p(r) = \frac{1}{2}\rho c U_0 \frac{a}{r} ka \tag{2.9}$$

which reveals a divergence at distances satisfying $\frac{r}{a} \gg 1$ and $\frac{r}{a} \gg ka$. Expression 2.8 reveals that the axial pressure exhibits strong interference effects, fluctuating between 0 and $2\rho c U_0$ as r changes between 0 and ∞. These extremes of pressure occur for values of r satisfying

$$\frac{1}{2}kr\left[\sqrt{1+\left(\frac{a}{r}\right)^2}-1\right]=m\frac{\pi}{2} \tag{2.10}$$

where maxima correspond to m odd, minima correspond m even. The expression 2.11 shows the values of r at the extrema,

$$\frac{r_m}{a}=\frac{1}{m}\frac{a}{\lambda}-\frac{m}{4}\frac{\lambda}{a} \tag{2.11}$$

The first local maximum in axial pressure is given by,

$$\frac{r_1}{a}=\frac{a}{\lambda}-\frac{1}{4}\frac{\lambda}{a} \tag{2.12}$$

For values of r greater than r_1, the axial pressure has a behaviour going from assymptotically to a $\frac{1}{r}$ dependence. For values below r_1, the axial pressure displays a strong interference effects, suggesting that the acoustic field close to the piston is complex. The distance r_1 serves as a convenient demarcation between this complex near field, close to the source, and the simpler far field situated at large distances from the source. The quantity r_1 has physical meaning only if the ratio $\frac{a}{\lambda}$ is large enough so that r_1 is positive. Indeed, if $a=\frac{\lambda}{2}$ then r_1 is zero and there is no near field. A sketch of this behaviour is shown in figure 2.3.

In order to guarantee the far field approximation, the signal wavelength and distance between the receivers and the loudspeakers were taken into account. The radius of the loudspeakers used in this work is around 4cm and the smaller wavelength used was 12.7cm, so $a<\frac{\lambda}{2}$, which assures the inexistence of the near field.

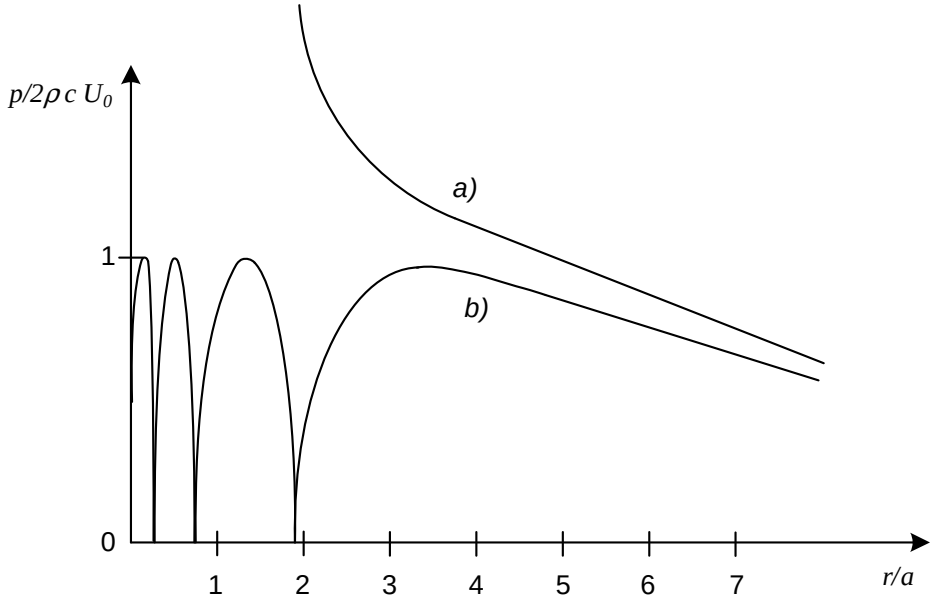

Figure 2.3 — On-axis response of a circular plane piston with $\frac{a}{\lambda} = 4$, a) eq. 2.9, b) eq. 2.8.

2.2.2 Directivity Pattern

The directional factor, $H(\theta)$ from the piston can be defined as

$$H(\theta) = \left| \frac{2J_1(ka\sin\theta)}{ka\sin\theta} \right| \tag{2.13}$$

where J_1 is the 1^{st} order Bessel function, k is the wave number, a the radius of the piston, and θ the angle relative to the perpendicular of the piston plane.

As the piston is mounted in an infinite baffle, the radiation is limited to the half space in front, i.e. to $\theta = \pm\frac{\pi}{2}$. Of course, if the case arises, a backward radiation without any interaction on the front radiation can be considered (but with a minus sign). A plot of $\frac{2J_1(ka\sin\theta)}{ka\sin\theta}$ is given in figure 2.4 where $u = ka\sin\theta$.

Because of the symmetry, only half the pattern is needed. When the radius of the piston is larger in comparison to the wavelength of the sound, $ka \gg 1$, the radiation pattern has many side lobes and the angular width of the major lobe is small. On the other hand, if the wavelength is much greater than the radius, then $ka \ll 1$ and only the major lobe will be present. The directivity pattern study

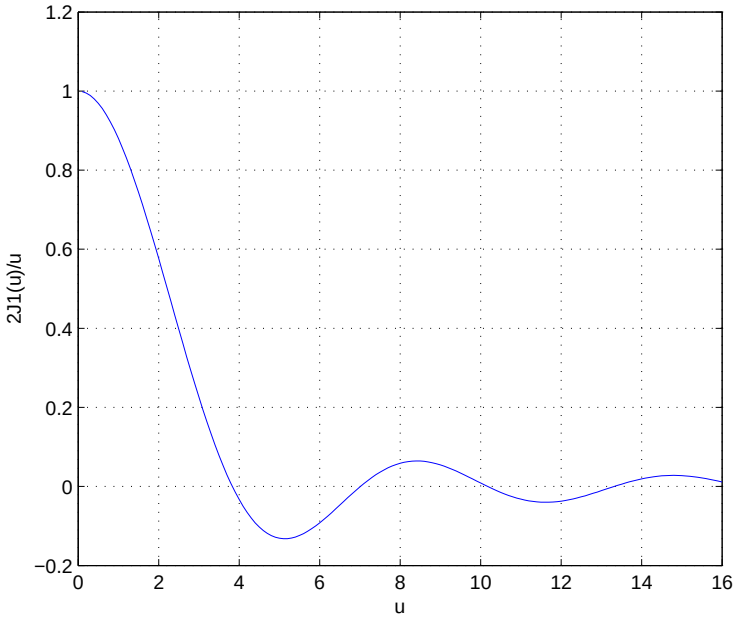

Figure 2.4 — Functional behaviour of $\frac{2J_1(ka\sin\theta)}{ka\sin\theta}$.

shows that the piston in a infinite baffle is practically not directive for $ka < 1$, i.e., when its circumference is smaller than the wavelength. For $ka > 2$, on the contrary, the directivity is pronounced, and for $ka = 3.83$ (first zero of J_1), side lobes appear. The radiation patterns produced by a piston-type loudspeaker differ to some extent from these idealized patterns. One reason for this discrepancy is that the area of the baffle in which the speaker is mounted is necessarily finite. At high frequencies even a baffle of small linear dimensions corresponds quite closely to an ideal infinite baffle but, at low frequencies, where the wavelength of the sound may be the same or greater than the linear dimensions of the baffle, this assumption cannot be considered.

On this work, the main subject is to assure the spherical pattern of the wave, once that in the spherical waves wavefronts are concentric spheres. In this sense, the phase signal has a linear behaviour with the distance to the source and does not depend of the angle θ, since the propagation is radial. The spherical wave pattern is guaranteed [Ros88] only in the case of a point source due to

the assumption of far field and the unidirectionality. The signal wavelengths considered are $13cm < \lambda < 66cm$, which corresponds to $1.93 < ka < 0.38$. These values of ka assure the predominance of the major lobe. The far field and the directivity pattern assures the spherical wave behaviour. The distance employed in this work (3 to 10 metres), contributes also to the assumption of point source.

Chapter 3

Hardware and Measurements

Summary: *This chapter discusses several characteristics about the hardware used in the implemented system and the pre-processing of the acquired data. It is, also, presented the most important phase combinations to solve this positioning problem.*

3.1 Equipment and Layout

This chapter is devoted to describe the equipment used, the signals transmitted and the pre-processing algorithms developed to track phases of the receiver signal. The goal is to compute the position of a receiver at an unknown location (usually called the roving receiver) using n transmitters and a receiver in a known fixed position by phase coherence analysis.

3.1.1 Sound Cards and Microphones

The hardware used to implement this system were loud speakers as transmitters and microphones as receivers, connected to standard computer source cards. The transmitters used were two 5.1 systems with a power rating of 6 watts RMS per speaker, providing a total of ten independent sound sources. The system has a signal-to-noise ratio of 75dB and a frequency response of 40Hz to 20kHz. Figure 3.1 shows the transmitters used in the experiment.

Figure 3.1 — Transmitter.

The two sound cards have 24-bit Digital-to-Analog conversion resolution and 16 or 24 bit Analog-to-Digital resolution with sampling rates of up to 48kHz in playback using 5.1 mode (up to 96kHz in stereo mode), and sampling rates up to 96kHz in recording.

The receivers used were two stereo microphones with sensitive electret

condensers. They have a bandwidth of 50Hz to 18kHz and sensitivity of −45dB. Figure 3.2 illustrates the reference receiver, attached to a tripod support.

Figure 3.2 — Reference Receiver.

3.1.2 Sound Waves

The acoustic signals used were composed of ten single frequency signals (sinusoids), one frequency per speaker, from 520Hz to 2710Hz with corresponding wavelengths from 66cm to 13cm. This band is attractive for several reasons. One is the fact that the aim of this work is to achieve centimetre-level accuracy, so the chosen wavelengths are larger than this accuracy figure, but small enough to allow the phase to be tracked to such accuracy. A phase measurement precision of a few hundreds of a wavelength can be expected out of processing a few periods at the noise levels that were used. Another reason stems from the fact that, in radio waves in the atmosphere, these wavelengths correspond to frequencies where broadcast stations (radio and TV) can be found. Table 3.1 shows the frequencies used.

In fact, it is desirable to employ lower frequencies and larger wavelengths for radio waves, to allow for easy building penetration (HF, VHF). The extremely higher propagation speed of radio waves compared to the frequency changes induced by the movement under measurement allows for the phase tracking loops to integrate over a significantly larger number of cycles, rendering better relative

Table 3.1 — Frequencies and respective wavelengths used in the system

Frequency (Hz)	Wavelength (cm)
520	66.19
625	55.07
750	45.89
902	38.16
1083	31.78
1301	26.46
1563	22.02
1878	18.33
2256	15.26
2710	12.70

accuracy. This allows for the use of larger wavelengths while obtaining similar accuracy figures.

All signals were sinusoids, as they are the most logical and simple signals of opportunity available. To avoid beat frequencies of two single frequencies signals around a third frequency in the admitted band, the frequencies were distributed according to a geometric progression. At least 100Hz can be allocated to each side of each frequency. As a matter of fact, only 25Hz needed to be guaranteed. This bandwidth is required to account for the rover motion, i.e. to account for the Doppler frequency shift due to motion, and also for the clock shifts between transmitters and receivers. Clock shifts of up to two parts per thousand, were considered.

The apparent frequency of a source increases or decreases depending on the motion of both source and receiver along the line between them. The frequency shift induced by a moving source is physically based on a change in the transmitted wavelength. On the other hand, the frequency shift induced by a moving receiver is physically based on a change in the receiver sound-wave speed.

Considering v_s and v_r the source and receiver speeds, and c the wave propagation speed, the frequency on the receiver is given by [AF99],

$$f' = f\left(\frac{c - v_r}{c - v_s}\right) \tag{3.1}$$

If v_r and v_s are small when compared with c, expression 3.1 can be written as,

$$f' = f\left(\frac{1}{c - v_{rs}}\right) \tag{3.2}$$

where $v_{rs} = v_r - v_s$. The experiments were performed with the source in a known and fixed position. So, in this particular case $v_{rs} = v_r$. After some mathematic manipulations, 3.2 is changed into,

$$\Delta f = -\frac{1}{\lambda} v_r \tag{3.3}$$

where $\Delta f = f' - f$.

It is assumed that the receiver velocity does not exceed 2.5m/s. In other words, the system was designed to measure receiver speeds of up to 2.5m/s without loss. This speed corresponds to fast walking or moderate running. Taking into consideration that the used signals wavelength is $0.1270m < \lambda < 0.6619m$ (shown in table 3.1) and that $v_r = 2.5m/s$, the induced frequency deviation is

$$4Hz < |\Delta f| < 20Hz \tag{3.4}$$

Therefore, the bandwidth required to account for rover motion is 20Hz. Assuming further 5Hz due to clock shifts (for the higher frequency), a total bandwidth of 25Hz was considered. This situation represents the limit to guarantee total phase recovery in all situations (except for noise effects).

This study can also be adapted to electromagnetic waves, in particular RF radiation. The difference between the Doppler Effect in sound and electromagnetic waves is more than the difference in wave speeds. That difference rises from the fact that the medium of propagation is removed (electromagnetic waves propagate in vacuum) and there is no longer a physical basis for the distinction between moving receiver and moving source. Besides the derivation of the

Doppler effects for electromagnetic radiation deal with the theory of special relativity, the frequencies used in this problem conduce to a classic problem which origins a similar expression to 3.2.

3.1.3 Physical Layout

As an initial study, the transmitter positions are an important parameter to define. The experimental setup was implemented in a room with sound absorbing capacity (anechoic chamber) and the transmitters were spread around the room. Figures 3.3 and 3.4 shows the configuration of the room.

Figure 3.3 — General view of the experimental setup.

After evenly spreading the transmitters around the experiment scenario and fixing the reference receiver, the positions of these elements were determined by a photographic survey. This analysis was based on methods of stereoscopic image comparison (photogrammetry) of several photos of the same objects taken from different locations and angles. These photos were taken by a digital camera; which was previously calibrated for lens distortion. The accuracy achieved by this

Figure 3.4 — Experimental setup.

method is related to the precision of the points marked on the photos (around 2cm). Figure 3.5 shows a schematic view of the transmitters and reference receiver locations. The transmitters were placed in locations with different levels and spread on xy-plane covering different directions, to guarantee good accuracy of the developed algorithm. The positions of the transmitters were computed considering a visible object in the processed photos as the origin of the orthogonal coordinate system.

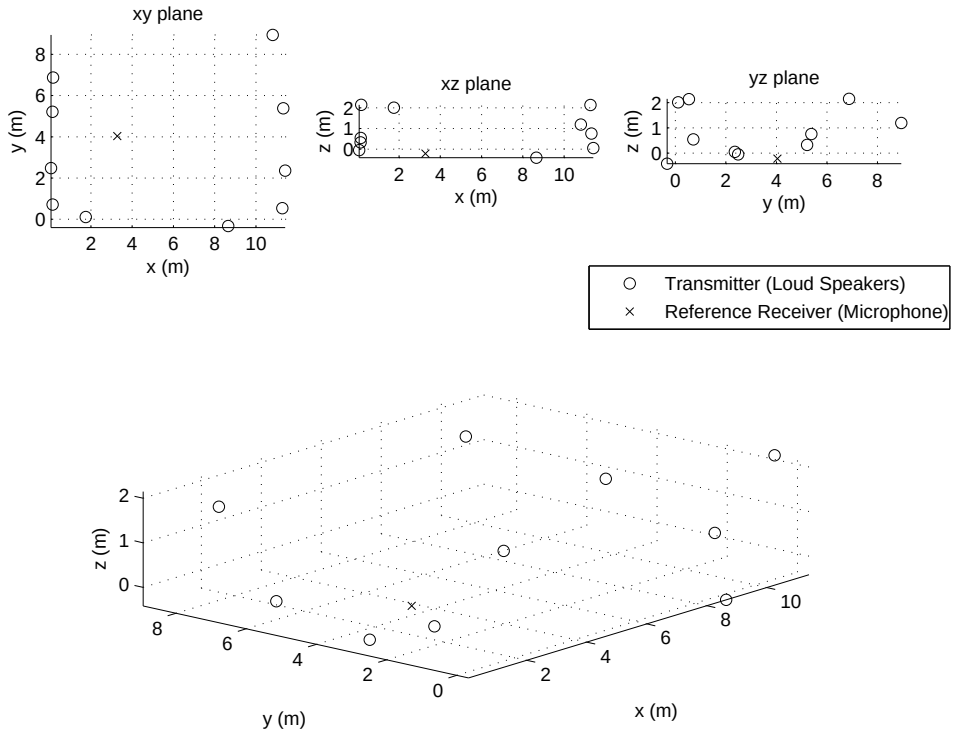

Figure 3.5 — Transmitters and reference receiver positions.

3.2 Phase Measurement Process

This section presents the data processing steps towards measuring the phase of the received signals. This pre-processing step converts the raw data collected by the receivers into instantaneous phase and amplitude estimates for each frequency from each transmitter.

3.2.1 Data Processing Definitions

A number of data processing definitions are relevant to the following discussion. A wave phase measured by a receiver in a specific position x and time t can be expressed, in cycles, by:

$$\phi(x,t) = \phi_0 + f_0(t - t_0) - \frac{d_{x_0}(x)}{\lambda_0} \tag{3.5}$$

where ϕ_0 is the initial phase of the transmitter at time t_0, $f_0(t-t_0)$ is the variation induced by frequency and $\frac{d_{x_0}(x)}{\lambda_0}$ is the phase variation induced by the distance $d_{x_0}(x)$ of the receiver at location x to the transmitter at location x_0. λ_0 is the wavelength: $\lambda_0 = c/f_0$, where c is the propagation speed, (340+0.6ΔT)m/s in the case of sound in the atmosphere, where ΔT is the temperature shift relative to 15°C. Equation 3.5 can be split into two expressions, as shown in 3.6,

$$\phi(x,t) = \phi_R(t) + \phi_M(t) \tag{3.6}$$

where ϕ_R is a reference phase generated by the receiver, which is composed by an initial phase ϕ_{R_0} and variation induced by frequency $f_{R_0}(t-t_0)$. So, ϕ_R is defined by,

$$\phi_R(t) = \phi_{R_0} + f_{R_0}(t-t_0). \tag{3.7}$$

$\phi_M(t)$ is the phase variation due to motion and frequency shifts between transmitter and receiver. The receiver collects samples of the received wave as in 3.5 and compares this signal with its own ϕ_R, computing the difference $\phi_M(t)$.

Disregarding amplitude, the transmitted signal is given by a sinusoidal wave expressed as follow,

$$x(t) = \sin(w_0 t + \phi_M(t)) \tag{3.8}$$

where $w_0 = 2\pi f_{R_0}$ is the angular frequency and f_{R_0} is the frequency of the transmitted signal.

To extract phase information, some mathematic manipulations are necessary. Multiplying 3.8 by $e^{iw_0t} = \cos(w_0t) + i\sin(w_0t)$ the expression obtained is, after trigonometric manipulations:

$$x(t)e^{iw_0t} = \frac{1}{2}[\cos(\phi_M(t)) - i\sin(\phi_M(t))] + \frac{1}{2}[\sin(2w_0t+\phi_M(t)) - i\cos(2w_0t+\phi_M(t))] \tag{3.9}$$

The second term of 3.9 can be eliminated through a low pass filter. Considering only the first term, the phase signal can be expressed by,

$$\phi_M(t) = \arctan\left(\frac{\sin(\phi_M(t))}{\cos(\phi_M(t))}\right) \tag{3.10}$$

3.2.2 Data Processing Parameters and Steps

This section describes the processing steps and some important parameters.

- The sound sampling rate was 44100Hz.
- The information considered has as a bandwidth of ±25Hz, which means that phase variations due to motion do not exceed this bandwidth. The speed of motion that induces Doppler frequency shifts was assumed to be lower than 2.5m/s, which correspond to fast walking or moderate running.
- The signal received from each microphone was multiplied by e^{iw_0t} for each angular frequency w_0 of each channel, as mentioned previously.
- The result was filtered by three cascaded low-pass finite impulse response (FIR) filters, each one followed by decimation to reduce processing effort.
    - The 1^{st} filter was applied at 44100Hz, had 32 coefficients, a pass band from 0Hz to 600Hz and a stop band from 4000Hz to Fs/2 with a maximum error on the pass band of ±0.5dB and a minimum attenuation on the stop band of -46dB. It was followed by a decimation factor of 5, producing a new sampling rate of 8820Hz;
    - The 2^{nd} filter was applied at 8820Hz, had 32 coefficients, a pass band from 0Hz to 70Hz and a stop band from 600Hz to Fs/2 with a maximum error on the pass band of ±0.12dB and a minimum attenuation on the stop band of 37dB. It was followed by a decimation factor of 7, producing a new sampling rate of 1260Hz;
    - The 3^{rd} filter was applied at 1260Hz, had 128 coefficients, a pass band from 0Hz to 25Hz and a stop band from 50Hz to Fs/2 with a maximum error on the pass band of ±0.15 and a minimum attenuation on the stop band of -57dB. It was followed by a decimation factor of 6, producing a new sampling rate of 210Hz;

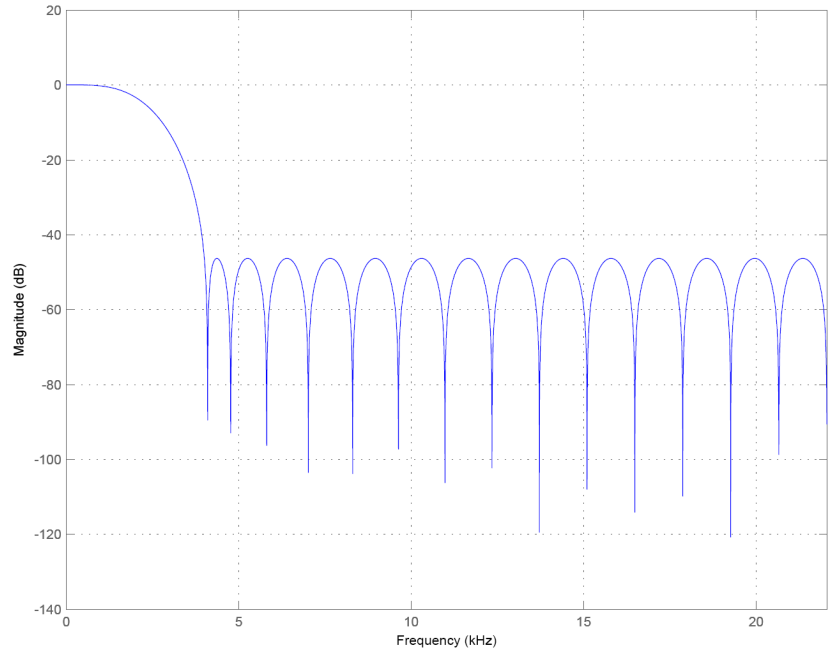

Figure 3.6 — FIR with a pass band from 0Hz to 600Hz and a stop band from 4000Hz.

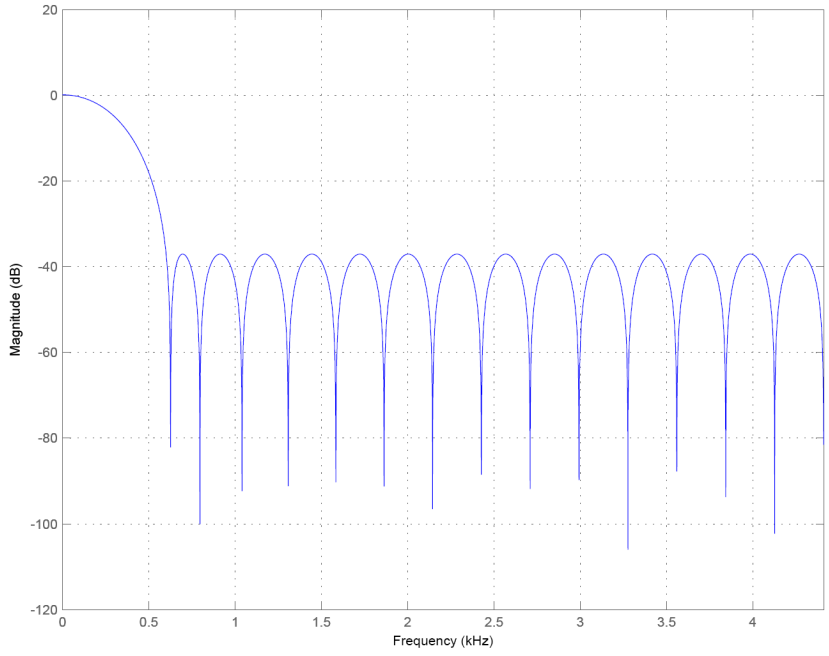

Figure 3.7 — FIR with a pass band from 0Hz to 70Hz and a stop band from 600Hz.

(Fs is the sampling rate for each case.)

Notice that the sampling frequency of each FIR is only slightly above twice

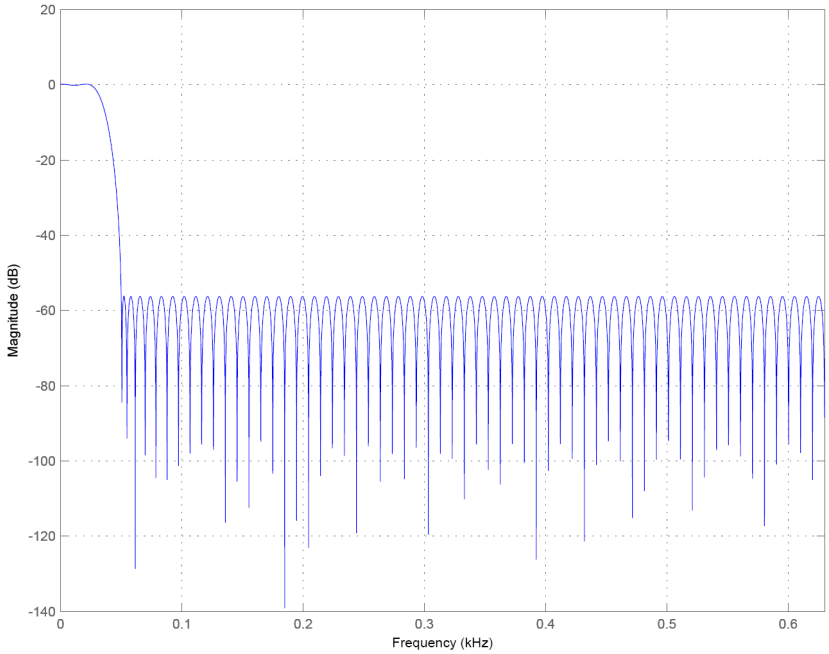

Figure 3.8 — FIR with a pass band from 0Hz to 25Hz and a stop band from 50Hz.

the start of the stop band of the previous FIR. The cascaded filter approach allows for significantly better computational efficiency when compared to a single filter. Using only one filter, the computational effort would be very high since the difference between the pass band and the stop band is very narrow compared with the sampling frequency. This would only be possible with a filter of a very high order.

- The resulting complex signal sampled at 210Hz was split into phase and magnitude. The former is the desired measurement; the latter is relevant to assess proper lock to the transmitted signal.

- Phase measurements were unwrapped to maintain the phase ambiguity constant since the last loss of lock. If it was not for motion and clock shifts, the phase measurements would always be constant. If cycle slips appear, phase information for positioning cannot be used, because the phase ambiguity is changed.

- Phase and magnitude have been further decimated by a factor of 21, con-

verting the sampling rate to 10Hz.

This last decimation does not respect the Nyquist criterion for a bandwidth of ±25Hz. However, the movements under consideration did not exceed this limitation and 10Hz was found to be more convenient, from a user point of view, for the procedures to follow. This sampling frequency does not affect the positioning results. The sampling rate could only alter the description of the trajectory. The motion spectrum cannot be all described with this sampling rate; however this value is higher than the sampling rates used by the common navigation systems.

This processing method was compared with an FFT processing method to assure the correct phase determination. This method consist of application of a Gauss sliding window of 4096 samples before computing FFT and determining the maximum frequency present in the signal and its neighbours. After computing the angle, this algorithm determines the differential phase compensation induced by the Gauss window and averages the extracted data to obtain the phase measurements. The position offset of the window was not considered because the signal is, by itself, the difference between two signals (so the computed phase is a relative value between two receivers). At last, this algorithm unwraps the values to obtain a continuous phase signal. The results were similar for all signals, which prove that the processing algorithm is suitable to the experiment. The use of a phase demodulator (using FIRs) has been considered to be more convenient, since it tracks efficiently phase signal and is also suitable for a real-time processing. Nevertheless, this processing method has a higher computational effort than the FFT method.

A FIR filter has linear phase, however it is important to check if processed phase signal corresponds exactly to the real signal. Some simulations were made to verify the behaviour of the linear phase FIRs used in this processing method. In the simulation has been considered a sinusoidal phase variation. Figure 3.9 shows the delay induced for this processing. Notice that signal amplitude, which

is the most important information, did not suffer any modification. Besides FIRs linear behaviour, it is induced a delay of an half of a sample. The delay induced by this method could be neglected since is equal for both receivers so, the phase difference processed is not affected.

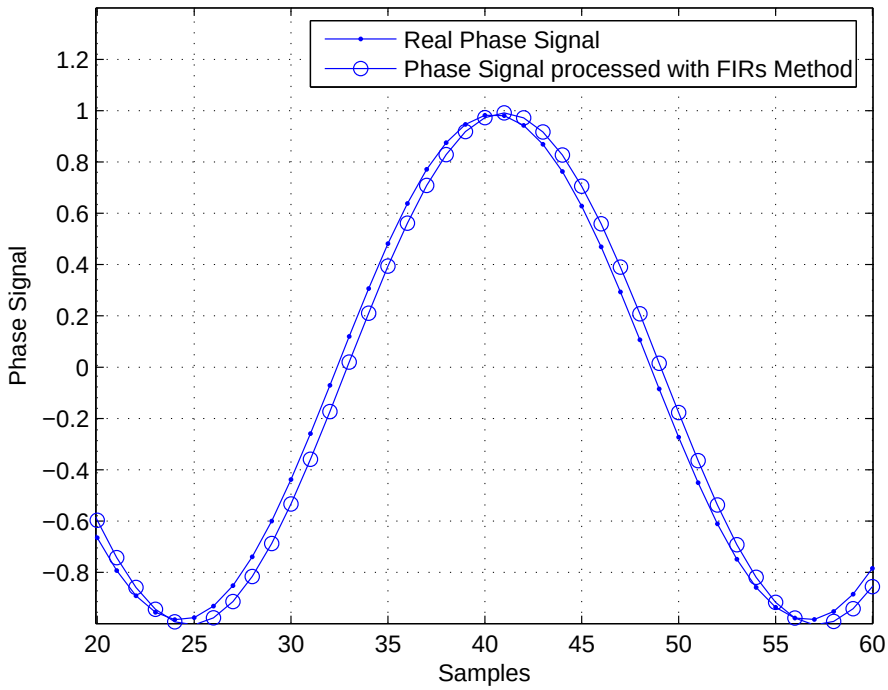

Figure 3.9 — Original phase signal and phase signal after processing.

3.3 Observables and Fundamental Combinations

The measurements recorded by the receiver represent the basic observables for the estimation of the relevant location parameters. The observation equations for phase may be used to form linear combinations in order to eliminate or reduce existing biases, as show in the sequel.

3.3.1 Carrier Phase

Considering a general situation with n transmitters, each of them generating the sinusoid of frequency f_i, (the transmitter i generates the frequency i), and two receivers [Hab99], the theoretical geometric distance between the transmitter i and the receiver k would be as expressed as in 3.11,

$$D_k^i = c\Delta\tau = c(t_k - t^i), \tag{3.11}$$

where c is the wave propagation velocity, $\Delta\tau$ is the propagation delay, t^i is the time of emission of the signal from transmitter i and t_k is the time of reception of the signal in receiver k. In fact, a measurement of this distance, using the phase values of the transmitted sinusoids, is biased due to the transmitter and receiver clock errors and due to an unknown integer number of cycles (ambiguity) between the transmitted and reference sinusoids, as introduced in 3.12,

$$d_k^i = c(\overline{t}_k - \overline{t}^i) + \lambda^i N_k^i, \tag{3.12}$$

where $\overline{t}^i$ is the reading of transmitter clock at time t^i and $\overline{t}_k$ is the reading of receiver clock at time t_k, λ^i is the wavelength of the i^{th} transmitter and N_k^i is the unknown integer number of cycles. The errors of the transmitter Δt^i and receiver Δt_k clocks are respectively,

$$\Delta t^i = \overline{t}^i - t^i, \tag{3.13}$$

$$\Delta t_k = \overline{t}_k - t_k. \tag{3.14}$$

Thus, the measured distance d_k^i can be written by 3.15,

$$d_k^i = D_k^i + c\Delta t_k - c\Delta t^i + \lambda^i N_k^i \tag{3.15}$$

where D_k^i is the geometric distance between transmitter i and receiver k, Δt_k and Δt^i are the receiver and the transmitter clock errors and $\lambda^i N_k^i$ are an unknown integer number of wavelengths. In fact, the geometric distance is unknown when the receiver is the rover: it depends on the rover position, which is precisely what

is sought to compute. As for the reference microphone, this distance has been measured by the photographic survey (section 3.1.3).

The phase of frequency i received by the receiver k can be expressed by 3.16,

$$\phi_k^i(\bar{t}_k) = \phi_0^i(\bar{t}^i) + N_k^i \tag{3.16}$$

with $\phi_k^i(\bar{t}_k)$ as the phase generated by receiver k for frequency i at time $\bar{t}_k$, $\phi_0^i(\bar{t}^i)$ as the phase generated by transmitter i and emitted at time $\bar{t}^i$ and N_k^i the unknown integer number of cycles (ambiguity). The basic phase difference observable, in metres, for transmitter i and receiver k may be written as shown in 3.17,

$$\Psi_k^i = \lambda^i(-\phi_k^i(\bar{t}_k) + \phi_0^i(\bar{t}^i) + N_k^i) \tag{3.17}$$

Introducing the clock errors Δt_k and Δt^i, 3.17 is changed into 3.18,

$$\Psi_k^i = \lambda^i(\phi_0^i(t_k - \Delta\tau + \Delta t^i) - \phi_k^i(t_k + \Delta t_k) + N_k^i) \tag{3.18}$$

After a Taylor series expansion around t_k, and considering only terms up to order one, due to the small magnitude of terms of higher order that could be neglected, 3.18 results in 3.19,

$$\Psi_k^i = \lambda^i(\Delta t^i f^i - \Delta\tau f^i - \Delta t_k f^i + N_k^i) \tag{3.19}$$

where f^i is the frequency of the signal produced by transmitter i. Through the relation $c = \lambda f$, the carrier phase is given by 3.20,

$$\Psi_k^i = \Delta t^i c - D_k^i - \Delta t_k c + \lambda^i N_k^i \tag{3.20}$$

where D_k^i is defined in equation 3.11. In cycles, the expression is 3.21,

$$\phi_k^i = \Delta t^i f^i - 1/\lambda^i D_k^i - \Delta t_k f^i + N_k^i \tag{3.21}$$

Expressions 3.20 and 3.21 are the fundamental equations that model the measurements from which the rover position will be computed.

3.3.2 Single Difference Phase Combination

Subtracting the measurement Ψ_l^i from transmitter i and receiver l, to measurement Ψ_k^i from the same transmitter and receiver k, assuming that transmitter i is almost simultaneously observed by the receivers, produces the single difference phase observable as expressed in 3.22,

$$\Delta\Psi_{kl}^i = \Psi_k^i - \Psi_l^i \tag{3.22}$$

substituting by 3.20, the single difference observable results in 3.23,

$$\Delta\Psi_{kl}^i = -\Delta t_{kl}c - D_{kl}^i + \lambda^i N_{kl}^i + \Delta t^i(\bar{t}_k) - \Delta t^i(\bar{t}_l) \tag{3.23}$$

with

$$\Delta t_{kl} = \Delta t_k - \Delta t_l \tag{3.24}$$

$$D_{kl}^i = D_k^i - D_l^i \tag{3.25}$$

$$N_{kl}^i = N_k^i - N_l^i \tag{3.26}$$

In this situation the transmitter clock error $\Delta t^i(\bar{t}_k) - \Delta t^i(\bar{t}_l)$ can be eliminated because $(\bar{t}_k - \bar{t}_l)$ is considerer to be small compared to the stability of the transmitter clock.

As a result, the single difference equation eliminates the transmitter clock error, as shown in equation 3.27. This justifies the need for a reference receiver.

$$\Delta\Psi_{kl}^i = -\Delta t_{kl}c - D_{kl}^i + \lambda^i N_{kl}^i \tag{3.27}$$

A navigation system that uses unsynchronised transmitters, like this one, must employ a reference receiver, (in other words, a reference microphone) at a fixed position. Otherwise, phase variation with time at a fixed position cannot be distinguished from phase variation caused by position change. Therefore, two microphones were used. One serves as a reference and is placed at a known location. The position of the other is determined from differences between the received signal phases locally and those received by the reference receiver.

3.3.3 Double Difference Phase Combination

The difference between two single difference observables of transmitter i and j leads to the double difference phase observable, as shown in 3.28,

$$\Delta\Delta\Psi_{kl}^{ij} = \Delta\Psi_{kl}^{i} - \Delta\Psi_{kl}^{j} \tag{3.28}$$

and results in 3.29,

$$\Delta\Delta\Psi_{kl}^{ij} = -D_{kl}^{ij} + \lambda^{i} N_{kl}^{i} - \lambda^{j} N_{kl}^{j} \tag{3.29}$$

where $D_{kl}^{ij} = D_{kl}^{i} - D_{kl}^{j}$.

By an analogous reason as with the single difference equation, the receiver clock term can be neglected (these terms are almost equals on both single difference observation equations, as the variation of the clock error in the interval between the reception of the signal from both transmitters is negligible).

This equation associates the observable $\Delta\Delta\Psi_{kl}^{ij}$ to the unknowns D_{kl}^{ij}, which is real and depends on the rover position, and the pair N_{kl}^{i}, N_{kl}^{j}, which are integer. This is the main equation used to compute the rover positions.

3.3.4 Triple Difference Phase Combination

Double difference phase observables from two different epochs t_1 and t_2 may be used to form the triple difference phase observable, as shown in 3.30,

$$\Delta\Delta\Delta\Psi_{kl}^{ij}(t_2, t_1) = \Delta\Delta\Psi_{kl}^{ij}(t_2) - \Delta\Delta\Psi_{ll}^{ij}(t_1) \tag{3.30}$$

If it is considered that the ambiguity parameters N_{kl}^{i} and N_{kl}^{j} do not change during the time interval $(t_2 - t_1)$ (which only occurs in the event of loss of lock or cycles slips during this interval), the phase ambiguities are eliminated and the observation equation results in 3.31,

$$\Delta\Delta\Delta\Psi_{kl}^{ij} = -(D_{kl}^{ij}(t_2) - D_{kl}^{ij}(t_1)) \tag{3.31}$$

The triple difference observable is used to calculate a good approximation of the relative position vector of the rover between epochs. Since there are more observations than unknowns, this equation is also useful for cycle slip detection.

Several algorithms were developed with single, double and triple observable equations. Triple difference phase combination is used to calculate the relative position vector between epochs, and double difference phase combination is decisive to determine the absolute rover positions. As said previously, double difference observable has two variables. One is real D_{kl}^{ij} and the others are integer, N_{kl}^{i} and N_{kl}^{j}. So, the expression to solve with double difference phase combination is in the form of,

$$y = Ax + Bz + v \tag{3.32}$$

where y is the phase signal, x is real and depends on rover position, z is integer and depends on an unknown integer number of wavelengths and v is the measurement noise.

The great challenge now is to solve equation 3.32 as a mixed real and integer weighted least squares optimization problem. This problem will be addressed in chapter 4 and chapter 5.

Chapter 4

Ambiguity Resolution

Summary: *This chapter presents the mathematics and algorithmics of integer parameter estimation for the implemented system.*

As explained in chapter 3, the carrier phase observation (equations 3.20 and 3.29 for single and double differences respectively) depends on real and integer parameters. The unknown integers are the number of carrier signal cycles of the difference between the transmitters and two receivers when the carrier phase is initially phase locked [AWWJ03].

4.1 Problem Statement

The linearized observation equation for double difference carrier phase measurement can be written as expressed in 3.32,

$$y = Ax + Bz + v$$

where $y \in \mathbb{R}^N$ is the observation vector, $x \in \mathbb{R}^p$ (real) and $z \in \mathbb{Z}^q$ (integer) are unknown vectors, A and B are known matrices with dimension $N \times p$ and $N \times q$ respectively and $v \in \mathbb{R}^N$ is the measurement noise which is assumed to be Gaussian with null mean and known covariance matrix W. In the specific problem of positioning, the dimension of the receiver position vector is p (which corresponds to $3\times$ number of epoch), q is the number of transmitters (number of transmitters-1 for double differences) and N is the number of equations.

The goal is to find and verify estimates of the unknown parameters x and z which maximize the likelihood of the residual v (measurement noise).

4.2 Estimation Problem

If $B = 0$ in the linearized observation equation for double difference phase measurements (equation 3.32), the least-squares method could be used to compute the estimate of x. However, this cannot be done in the presence of an integer variable. In order to obtain estimates of both variables, x and z, the maximum likelihood (ML) estimation is divided into computing x given z, and

z separately [HB98]. The ML estimates of x and z are found by maximizing the probability of observing y given x and z, i.e. by definition expressed in 4.1,

$$(x_{ML}, z_{ML}) = \max_{x\in\mathbb{R}^p, z\in\mathbb{Z}^q} P_{y|x,z}; (x, z) \in \mathbb{R}^p \times \mathbb{Z}^q \tag{4.1}$$

Since v is Gaussian with zero mean and covariance W, the probability density of y given x and z is also Gaussian with mean $Ax + Bz$ and covariance W. The maximum of this quantity can be found by minimizing 4.2,

$$(x_{ML}, z_{ML}) = \min_{x\in\mathbb{R}^p, z\in\mathbb{Z}^q} \|y - Ax - Bz\|^2_{W^{-1}} \tag{4.2}$$

which is similar to,

$$(x_{ML}, z_{ML}) = \min_{x\in\mathbb{R}^p, z\in\mathbb{Z}^q} (y - Ax - Bz)^T W^{-1} (y - Ax - Bz) \tag{4.3}$$

Equation 4.3 can be expressed as,

$$(x_{ML}, z_{ML}) = \min_{x\in\mathbb{R}^p, z\in\mathbb{Z}^q} \left[W^{-1/2}(y - Ax - Bz)\right]^T \left[W^{-1/2}(y - Ax - Bz)\right] \tag{4.4}$$

once that $W^{-1} = (W^{-1/2})^T W^{-1/2}$. The multiplication by W^{-1} produces a Normal noise, i.e., $\mathbb{E}\left(\mu\mu^T\right) = I$ where $\mu = W^{-1/2}\left(y - Ax - Bz\right)$.

Expanding 4.3, and completing the squares after adding and subtracting the terms $y^T A(A^T W^{-1} A)^{-1} A^T (Ax + Bz - y)$ and $z^T B^T A(A^T W^{-1} A)^{-1} A^T (Ax + Bz - y)$, the following equation is obtained,

$$(x_{ML}, z_{ML}) = \min_{x\in\mathbb{R}^p, z\in\mathbb{Z}^q} \left[(x - \hat{x}_{|z})^T Q^{-1} (x - \hat{x}_{|z}) + (z - \hat{z})^T T^{-1} (z - \hat{z}) + y^T \Delta y\right] \tag{4.5}$$

where $\hat{x}_{|z}$ is the estimate of x given z given by

$$\hat{x}_{|z} = QA^T W^{-1}(y - Bz), \tag{4.6}$$

Q is the covariance matrix of $\hat{x}_{|z}$ with expression,

$$Q = (A^T W^{-1} A)^{-1}, \tag{4.7}$$

$\hat{z}$ is the estimate of z as a real number and T is the covariance matrix of $\hat{z}$

$$T = (B^T W^{-1}(W - AQA^T)W^{-1} B)^{-1} \tag{4.8}$$

The term $y^T \Delta y$ does not depend on x or z and, therefore, does not affect x_{ML} and z_{ML}. The minimization of this equation produces estimates of x and z, which are called the floating solutions as x_{ML} and z_{ML}, because these estimates are real numbers. Notice that the $rank(A)$ has to be at least equal to the number of columns, p, for an determined system of equations, i.e. $rank(A) = p$. In the general case, where $y = [AB]\,[xz]^T$, the $rank([AB]) = p + q$ for a possible system of equations, which means that the number of linearly independent equations has to be equal to $p + q$. If this condition was not verified, then the system is underdetermined.

Per equation 4.5, this problem can be separated into two least-squares problem: one regarding minimization of $(z - \hat{z})^T T^{-1}(z - \hat{z})$ on $z \in \mathbb{Z}^q$ followed by the minimization of $(x - \hat{x}_{|z})^T Q^{-1}(x - \hat{x}_{|z})$ on $x \in \mathbb{R}^p$ (notice that $\hat{x}_{|z}$ depends on the result z of the first minimization). The challenging problem is to find the integer z that solves the first problem. This problem of integer minimization can be stated in expression 4.9,

$$z_{ML} = \min_{z \in \mathbb{Z}^q} \left[((z - \hat{z})^T T^{-1}(z - \hat{z}) \right] \tag{4.9}$$

Cleary, the minimum over a real vector space is zero when z is equal to $\hat{z}$. The aim is to find an integer vector z which is close to $\hat{z}$. A simple and naïve approach is to round each component of $\hat{z}$ to its nearest integer. This simple approach would work if T were diagonal (or nearly diagonal). However, in practice, this is not the case, as ambiguities are coupled by 4.8.

Once the minimum over $z \in \mathbb{Z}^q$ is found, the maximum likelihood estimate of x is found by substituting z into the least-squares equation. The expression obtained is expressed in 4.10,

$$x_{ML} = \hat{x}_{|z} = (A^T W^{-1} A)^{-1} A^T W^{-1}(y - Bz) \tag{4.10}$$

Considering $\hat{z}$ as a random variable on true z ($\in \mathbb{Z}^q$), it is clear that its distribution is Gaussian with mean z and covariance T: $\hat{z}$ is a linear function of Gaussian

variable y. The probability distribution of $\hat{z}$ suggests that,

$$\hat{z} = z + u \tag{4.11}$$

where u is Gaussian with zero mean and covariance matrix T ($u \sim N(0, T)$). Multiplying both sides by $G = T^{-1/2}$ and by defining $\widetilde{y} = G\hat{z}$, equation 4.11 is equivalent to,

$$\widetilde{y} = Gz + \bar{u} \tag{4.12}$$

where $\bar{u}$ is a Gaussian random variable with zero mean and unit variance. Notice that $T^{-1/2} = (T^{-1})^{1/2}$ where the $M^{1/2}$ is any square matrix S such that $S^T S = M$. If M is strictly positive definite, S is non-singular.

Expression 4.9 can be written in an equivalent form, as expressed in 4.13,

$$z_{ML} = \min_{z \in \mathbb{Z}^q} \|\widetilde{y} - Gz\|^2 \;\; z \in \mathbb{Z}^q \tag{4.13}$$

The set $\{Gz | z \in \mathbb{Z}^q\}$ is a lattice in $\mathbb{R}^q$. This equation suggests that the maximum likelihood value of z is found by computing the point of the lattice that is closest to vector $\widetilde{y} \in \mathbb{R}^p$.

4.2.1 Lattices and Basis Reduction

As said, $L(G) = \{Gz | z \in \mathbb{Z}^q\}$ is the lattice generated by G, where G is any matrix with real entries whose rows are linearly independent. The rows of G are called a basis of L and the number of vectors q (columns of G) is said to be the dimension of the lattice L.

The Voronoi region or a Voronoi cell of a lattice point is the set of all points closer to Gz than any other point in the lattice. It is obvious from equation $\widetilde{y} = Gz + \bar{u}$ that $\widetilde{y}$ is off from Gz by $\bar{u}$. So, if $\bar{u}$ is small enough that $\widetilde{y}$ remains in the Voronoi cell of lattice point Gz, the estimate of z is correct. Because of the periodic structure of the lattice, the Voronoi cell of Gz is the translation of the Voronoi cell of the origin V_0 by the vector Gz. The Voronoi diagram of a lattice is the set of all its Voronoi regions [SL04].

To better understand these definitions, consider the following lattice generator matrix (equation 4.14) as an example:

$$G_1 = \begin{bmatrix} 1 & 0 \\ 0 & 1 \end{bmatrix} \tag{4.14}$$

The rows of G_1 $\begin{bmatrix} 1 & 0 \end{bmatrix}$ and $\begin{bmatrix} 0 & 1 \end{bmatrix}$ are the base vectors as shown in figure 4.1. The Voronoi cells for the same lattice are shown as the thick square blocks in figure 4.2. All Voronoi cells are translations of the cell at origin, which is shown by the shaded region. Note that the basis vectors for this lattice are orthogonal to each other and, for a given floating point, the nearest lattice point can be found by simply rounding it to the nearest integer.

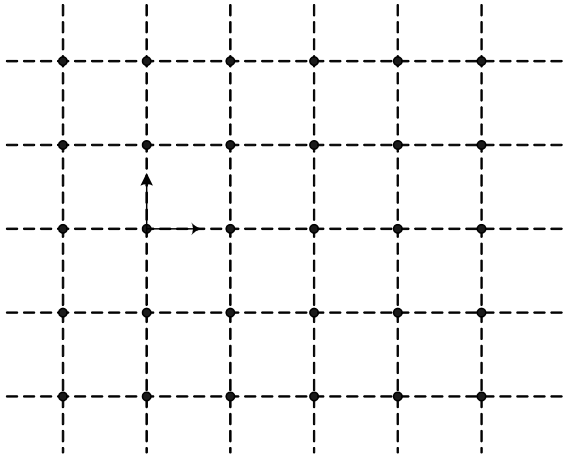

Figure 4.1 — Basis vector for a square lattice.

Two lattices are said to be identical if all lattice points are the same in $\mathbb{R}^n$. Two generator matrices G_1 and G_2 generate identical lattices $L(G_1)$ and $L(G_2)$ if and only if there is an integer combination of the columns of G_1 (basis of $L(G_1)$) that generates the columns of G_2 and vice-versa. Such relationship is equivalent to the existence of F such that,

$$G_2 = G_1 F \tag{4.15}$$

where F is a square matrix with integer entries such that $|detF| = 1$ (which is a necessary and sufficient condition for F^{-1} to be integer). This matrix can be seen from an isomorphism from $\mathbb{Z}$ onto $\mathbb{Z}$.

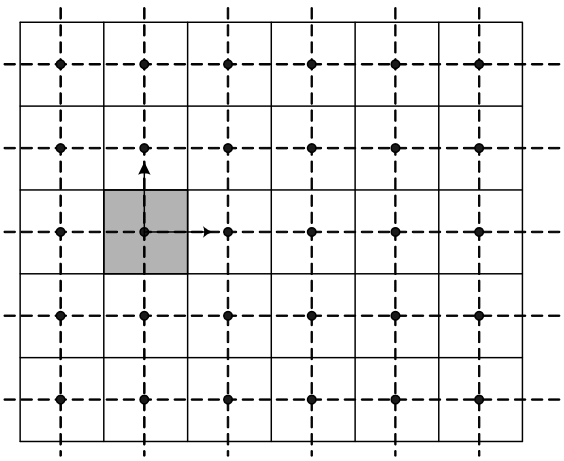

Figure 4.2 — Voronoi cell for a square lattice.

Now consider another generator matrix in 4.16

$$G_2 = \begin{bmatrix} 2 & 1 \\ 1 & 1 \end{bmatrix} \tag{4.16}$$

This matrix can be written in the form of

$$G_2 = \begin{bmatrix} 2 & 1 \\ 1 & 1 \end{bmatrix} = \begin{bmatrix} 1 & 0 \\ 0 & 1 \end{bmatrix} \begin{bmatrix} 2 & 1 \\ 1 & 1 \end{bmatrix} = G_1 F$$

Since F contains integer entries and $|detF| = 1$, lattices generated by G_1 and G_2 are identical. The lattice generated by G_2 with its base vectors and Voronoi regions is shown in figure 4.3. Note that the basis vectors for generator matrix G_2 are not orthogonal to each other. Hence, finding the nearest lattice point problem is no longer a simple task. Consider a real point in the space as shown in figure 4.4. The nearest lattice point is point 1, but rounding to the nearest integer will give point 2, which is not the correct solution.

It is evident from this example that the nearest lattice point can be obtained easily only if the basis vectors are orthogonal (or almost orthogonal). For the purpose of solving 4.13, it is advantageous to have reasonably orthogonal basis vectors and as homogeneous as possible. The process of selecting good basis for a given lattice, given some criteria, is called reduction. In section 4.2.3 one of these methods will be discussed.

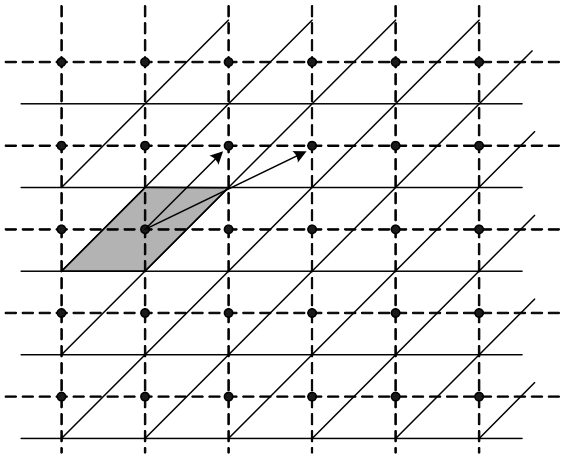

Figure 4.3 — Lattice generated by generator matrix G_2.

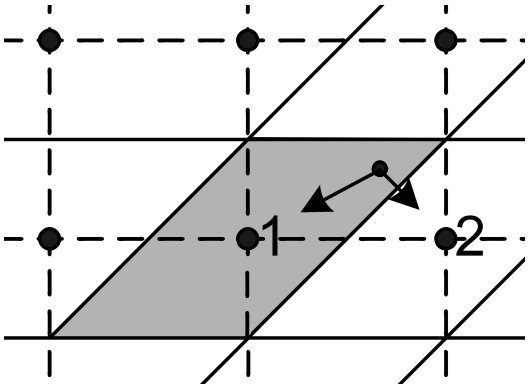

Figure 4.4 — Round-off may not yield correct solution when lattice is not orthogonal.

4.2.2 Searching for integer points inside an ellipsoid

After one or more suboptimal solutions to the integer least-squares problem has been found, it is necessary to check whether these solutions are probabilistically reasonable or not. This verification uses the fact that the residual error $\bar{u}$ in 4.13 has normal distribution: it corresponds to checking that $\bar{u}$ lies inside an ellipsoid that limits the volume of a given probability of $\bar{u} \sim N(0, I)$.

The ellipsoid ϵ is given by expression 4.17

$$\begin{gathered} \epsilon = \{\bar{z} | \bar{z} \in \mathbb{R}^q, \|\widetilde{y} - G\bar{z}\| < r\} \\ or \\ \epsilon = \left\{\bar{z} | \bar{z} \in \mathbb{R}^q, (\bar{z} - \hat{z})^T T^{-1} (\bar{z} - \hat{z}) < r^2\right\} \end{gathered} \tag{4.17}$$

where $\bar{z}$ is the set of all real values. The goal of this study is to find at least one integer point ($z \in \mathbb{Z}^q$) inside the region expressed in 4.17. The easiest way of finding integer points inside ϵ is finding the minimum volume box covering an ellipsoid. Figure 4.5 shows a two dimensional model.

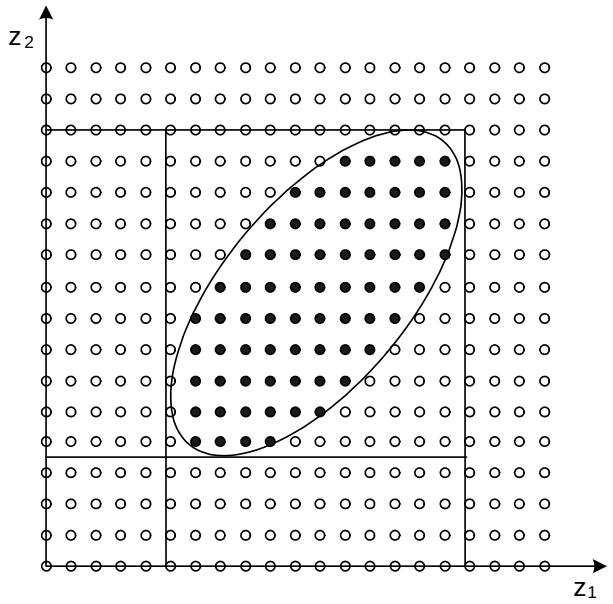

Figure 4.5 — The minimum volume box covering the ellipsoid ϵ.

In fact, this kind of approximation could be very conservative if the axis of the ellipsoid are not parallel to the coordinate axes, which is the same as T being far from diagonal. It is important to reach these criteria to have a good estimate. Again, reduction of the lattice is used to get almost orthogonal G (diagonal T). The minimum volume box covering the ellipsoid is hopefully a good approximation to the ellipsoid and contains fewer integer points satisfying 4.17.

As said previously, the reduction method limits the search region. As a result, this method gives a set of solutions and respective probabilities. In a well tuned process, the probability of the most favourable solution will be close the unit and will be correct.

4.2.3 Lenstra, Lenstra, Lovász (LLL) Algorithm

The process of selecting a good basis for a given lattice, given some criterion, is called reduction. The LLL algorithm is one if these methods [HMK98], that orthogonalize matrix G as much as possible, while preserving the lattice structure. As mentioned before, in this problem, it is advantageous if the basis vectors are as short as possible and reasonably orthogonal to each other. With the LLL algorithm, an n-dimensional reduction problem can be recursively reduced to an $(n-1)$-dimensional reduction problem. Suppose a lattice $L = L(G)$ and let G be a $(n \times q)$, $n \geq q$, matrix given by $G = \begin{bmatrix} g_1 & g_2 & \dots & g_q \end{bmatrix}$. A reduced basis is obtained given the following steps:

- Perform the Gram-Schmidt orthogonalization, denoted by $\begin{bmatrix} g_1^* & g_2^* & \dots & g_q^* \end{bmatrix}$ where,

$$g_1 = g_1^* \qquad g_k^* = g_k - \sum_{j=1}^{k-1} \mu_{kj} g_j^* \tag{4.18}$$

  with

$$\mu_{kj} = \frac{g_k^T \cdot g_j^*}{g_j^* \cdot g_j^*} \tag{4.19}$$

- For $k = 1, 2, \dots, q$, and, given k, for $j = 1, 2, \dots, k-1$, replace g_k by $g_k - \lceil \mu_{kj} \rfloor \, g_j$ where $\lceil \mu_{kj} \rfloor$ is the integer closest to μ_{kj};

- Update the g_k^*s and μ_{kj}s according to 4.18 and 4.19;

- If there is a subscript k violating

$$\left\| g_{k+1}^* + \mu_{(k+1)k} g_k^* \right\|^2 \geq \frac{3}{4} \left\| g_k^* \right\|^2 \tag{4.20}$$

  then swap g_k^* and g_{k+1}^* and return to the first step; otherwise stop.

Chapter 5

Developed Algorithms

Summary: *This chapter describes several algorithms developed with different phase combinations to solve the addressed positioning problem.*

Several algorithms were developed to achieve the purpose of this dissertation: tracking a rover receiver through phase processing of the acoustic acquired signal. Although other algorithms were developed, this chapter describes only the most important and final algorithms.

5.1 Ambiguity Resolution

In order to determine the position of the receiver, an algorithm that finds the most probable rover receiver position for each epoch was designed. This algorithm is based on observables 3.29 and consists on an efficient procedure to compute a feasible set of admissible ambiguities and related rover positions through probabilistic analysis. Since the term D_{kl}^{ij} in 3.23 is a function of the rover position, 3.29 can be expressed by:

$$\Delta\Delta\Psi_{kl}^{ij} = -D_{kl}^{ij}(x_k) + \lambda^i N_{kl}^i - \lambda^j N_{kl}^j, \tag{5.1}$$

where $D_{kl}^{ij}(x_k) = D_k^{ij} - D_l^{ij}(x_k)$. Considering the rover as the receiver k, $D_k^i(x_k)$, after a Taylor series expansion, is,

$$D_k^i(x_k) = D_k^i(x_0) + \left.\frac{\partial D_k^i}{\partial x}\right|_{x_0} (x_k - x_0) \tag{5.2}$$

with x_0 as an initial estimate of rover position. $D_{kl}^{ij}(x_k)$ can be defined as,

$$D_{kl}^{ij}(x_k) = D_k^{ij}(x_0) + \left(\left.\frac{\partial D_k^i}{\partial x}\right|_{x_0} - \left.\frac{\partial D_k^j}{\partial x}\right|_{x_0} \right) (x_k - x_0) - D_l^{ij} \tag{5.3}$$

The double difference equation can be written as,

$$\Delta\Delta\Psi_{kl}^{ij} - D_l^{ij} + D_k^{ij}(x_0) = -\left(\left.\frac{\partial D_k^i}{\partial x}\right|_{x_0} - \left.\frac{\partial D_k^j}{\partial x}\right|_{x_0} \right) (x_k - x_0) + \lambda^i N_{kl}^i + \lambda^j N_{kl}^j + v \tag{5.4}$$

where $(x_k - x_0)$ is the real variable, N_{kl}^i and N_{kl}^j are the integer variables and v is the measurement noise.

As far as the subtraction of one transmitter, i, to the other, j, is concerned, instead of using metres, number of cycles were adopted as units (the difference

rises from the fact that $f_i \neq f_j$). In cycles, equation 5.4 can be expressed as follows,

$$\Delta\Delta\phi_{kl}^{ij} + \frac{1}{\lambda^i}(D_k^i(x_0) - D_l^i) - \frac{1}{\lambda^j}(D_k^i(x_0) - D_l^j) =$$
$$= -\left(\frac{1}{\lambda^i}\frac{\partial D_k^i}{\partial x}\bigg|_{x_0} - \frac{1}{\lambda^j}\frac{\partial D_k^j}{\partial x}\bigg|_{x_0}\right)(x_k - x_0) + N_{kl}^{ij} - (f^i - f^j)(\Delta t_k - \Delta t_l) + v \quad (5.5)$$

Notice that this expression has a time dependence that does not exist in the same expression in metres. However, in this work, $(f^i - f^j)(\Delta t_k - \Delta t_l)$ can be neglected because the error induced by $(\Delta t_k - \Delta t_l)$ is assumed to be small. This happens due to the minimization of the clock errors achieved by the hardware used. This term can be neglected only if $(\Delta t_k - \Delta t_l)$ is, at least, an order of magnitude inferior to the wave speed that this problem deal with. The error induced by $(\Delta t_k - \Delta t_l)$ is of the same order of magnitude of the light speed. In this case, sound speed is lower than the error induced by $(\Delta t_k - \Delta t_l)$. So, the expression used in this study is,

$$\Delta\Delta\phi_{kl}^{ij} + \frac{1}{\lambda^i}(D_k^i(x_0) - D_l^i) - \frac{1}{\lambda^j}(D_k^i(x_0) - D_l^j =$$
$$= -\left(\frac{1}{\lambda^i}\frac{\partial D_k^i}{\partial x}\bigg|_{x_0} - \frac{1}{\lambda^j}\frac{\partial D_k^j}{\partial x}\bigg|_{x_0}\right)(x_k - x_0) + N_{kl}^{ij} + v \quad (5.6)$$

Again, this expression has two variables. One is real $(x_k - x_0)$ and the other is an integer variable N_{kl}^{ij}. As said previously, the expression to be solved is,

$$y = Ax + Bz + v \quad (5.7)$$

where $A = \left(\frac{\partial D_k^i}{\partial x}\Big|_{x_0} - \frac{\partial D_k^j}{\partial x}\Big|_{x_0}\right)$ and B is the identity matrix.

In the case of RF signals, whose wave velocity is the speed of light, the error induced by $(\Delta t_k - \Delta t_l)$ and the wave speed have the same order of magnitude, so they cannot be neglected. Considering that $(\Delta t_k - \Delta t_l)$ is not negligible and using the double difference equation in metres (equation 5.4), the result is also composed by two variables, a real variable given by $(x_k - x_0)$, and an integer variable which is $(\lambda^i N_{kl}^i + \lambda^j N_{kl}^j)$. According to the expression 5.7,

$$A = \left(\frac{\partial D_k^i}{\partial x}\bigg|_{x_0} - \frac{\partial D_k^j}{\partial x}\bigg|_{x_0}\right)$$

and

$$B = \begin{bmatrix} -\lambda^i & \lambda^j & 0 & \dots & \lambda^n \\ -\lambda^i & 0 & \lambda^k & \dots & \lambda^n \\ \vdots & \vdots & \vdots & \ddots & \vdots \\ -\lambda^i & 0 & 0 & \dots & \lambda^n \end{bmatrix}$$

for each epoch and bearing in mind the differences between transmitters as $n-i$, where i is the transmitter which emits the signal with higher wavelength and n is the n^{th} transmitter.

After identified all terms in expression 5.7, the ambiguity resolution algorithm computes separately the maximum likelihood estimation of z and x, as addressed in chapter 4. This problem is solved considering two least-squares problems. One regarding minimization of the integer variable followed by the minimization of the real variable, taking into account that real variable, x, depends on the result of the integer variable minimization. This expression (equation 4.5) is shown below,

$$(x_{ML}, z_{ML}) = \min_{x \in \Re^p, z \in Z^q} \left[(x - \hat{x}_{|z})^T Q^{-1} (x - \hat{x}_{|z}) + (z - \hat{z})^T T^{-1} (z - \hat{z}) + y^T \Delta y \right]$$

The problem of integer estimation, which is stated on 4.9, consists on finding an integer vector z which is close to the floating solution $\hat{z}$ of the first minimization. A simple way to determine the integer variable z is round $\hat{z}$ to its nearest integer. Nevertheless, this cannot be done since ambiguities are coupled, which means that basis vectors are not orthogonal. The method of lattice reduction, LLL algorithm (section 4.2.3), orthogonalize as much as possible the basis, which involves a change of basis on z. As a result, this method gives a set of solutions and respective probabilities by rounding $\hat{z}$ described in the new basis, which is almost orthogonal.

The real variable estimation is now found by substituting z into the least-squares minimization, which is explained, in detail, on chapter 4.

From this algorithm is determined the most probable rover location for a

specific epoch. This algorithm has a high computational effort. From this point of view, it is highly inefficient determine rover position for all epochs with it. This algorithm, by itself, is not suitable for a real-time application due to its high processing effort.

5.2 Triple Difference Phase Algorithm

This algorithm computes the rover receiver position for each epoch, assuming that ambiguity parameters do not change during the time interval between epochs. In this way, the algorithm will be able to describe the rover route for any given initial position (which is supplied as argument). Considering equation 3.30 and assuming that the ambiguity parameters do not change in the given time interval, the expression obtained is,

$$\Delta\Delta\Delta\Psi_{kl}^{ij} = -(D_{kl}^{ij}(x_{m+1}) - D_{kl}^{ij}(x_m)) \tag{5.8}$$

where $D_{kl}^{ij}(x_m)$ is the distance between the pair of receivers and the transmitters for the position at epoch t_m and $D_{kl}^{ij}(x_{m+1})$ is the distance between the receiver pair and the transmitters for the position at epoch t_{m+1}. $D_{kl}^{ij}(x_{m+1})$ is unknown but the prediction can be obtained by a Taylor series expansion, as expressed in 5.9,

$$D_{kl}^{ij}(x_{m+1})_s = \left.\frac{\partial D_{kl}^{ij}}{\partial x}\right|_{(x_{m+1})_{s-1}} \Delta x + D_{kl}^{ij}(x_{m+1})_{s-1} \tag{5.9}$$

where $\Delta x = (x_{m+1})_s - (x_{m+1})_{s-1}$ is the position variation and s is the s^{th} iteration necessary to converge where in the first iteration, $s = 1$, the algorithm assumes $(x_{m+1)})_0 = x_m$. These iterations are responsible for the linearization errors minimization.

So, equation 5.8 is changed into 5.10,

$$\Delta\Delta\Delta\Psi_{kl}^{ij} = \left.\frac{\partial D_{kl}^{ij}}{\partial x}\right|_{(x_{m+1})_{s-1}} \Delta x + D_{kl}^{ij}(x_{m+1})_{s-1} - D_{kl}^{ij}(x_m) \tag{5.10}$$

(It corresponds to

$$\Delta\Delta\Delta\Psi_{kl}^{ij} = \left.\frac{\partial D_{kl}^{ij}}{\partial x}\right|_{(x_{m+1})_{s-1}} \tag{5.11}$$

for the 1^{st} iteration.) Δx can be computed as the minimum quadratic error, like expressed in 5.12,

$$\left.\frac{\partial D_{kl}^{ij}}{\partial x}\right|_{(x_{m+1})_{s-1}} \Delta x = D_{kl}^{ij}(x_{m+1})_s - D_{kl}^{ij}(x_{m+1})_{s-1} \tag{5.12}$$

The receiver position can now be calculated by,

$$(x_{m+1})_s = (x_{m+1})_{s-1} + \Delta x \tag{5.13}$$

Figure 5.1 shows the rover trajectory on the horizontal plane, with a quasi-constant height of about 30 cm below the reference receiver. The motion was obtained a walking person holding the microphone. A few points were marked as a reference for the rover trajectory. A track was performed around these points.

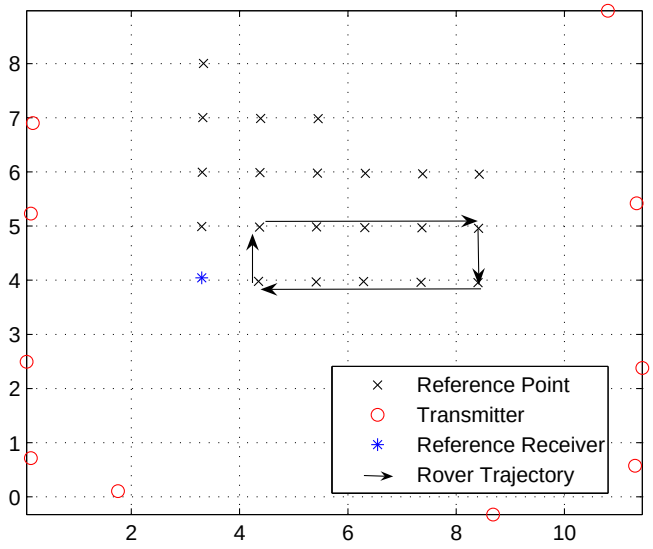

Figure 5.1 — Schematic view of the rover course.

Figure 5.2 shows the results obtained with the triple differences algorithm. Views from different planes are shown, as well as one perspective view of the entire trajectory. As can be seen in figure 5.2, the results using this algorithm describe the course on the horizontal plane correctly. Nevertheless, there is a drift in the vertical plane. This error on the vertical plane may have been originated by errors in the initial position estimates. As has already been mentioned, this algorithm starts with a rover position which is roughly estimated. The presence of undetected cycle slips and the errors accumulated from one epoch to the following contributes also for this drift.

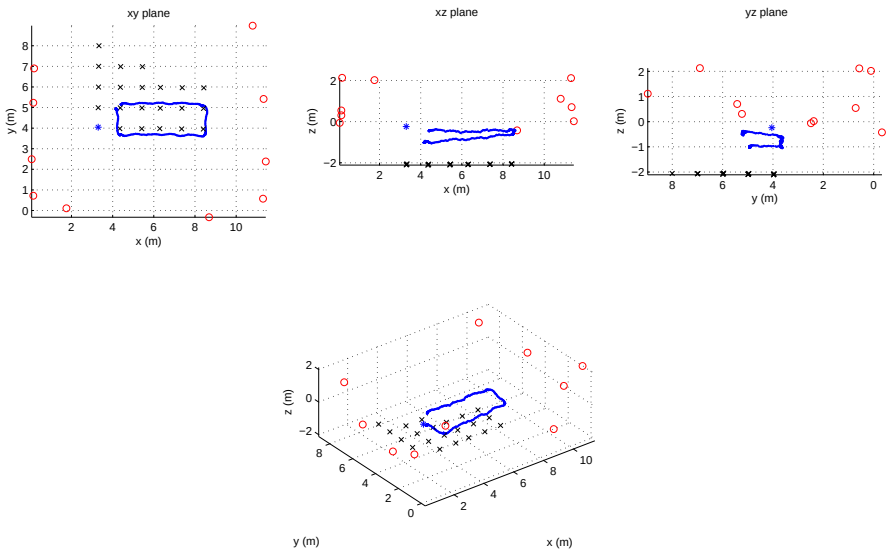

Figure 5.2 — Acquired and processed data with triple difference phase algorithm.

This algorithm, by itself, is unable to compute the absolute rover location. However, it is extremely useful to predict the rover location for several epochs, without the need for ambiguity resolution algorithms for all time instants. As addressed in section 5.1 the ambiguity resolution algorithm demands a high computational effort.

5.3 Positioning Algorithm

The algorithms previously described, by themselves, do not solve the navigation problem. For an efficient solution of this problem it was necessary to join the two algorithms previously presented. The new algorithm computes the double difference position solution with ambiguity resolution (section 5.1) by blending several epochs through triple difference phase algorithm (section 5.2).

The information of more than one epoch paves the way for determining the rover position. This information increases the number of equations in the system, but roughly maintains the number of integer variables. A set of N equations and 3 real variables is introduced at each epoch, where N is the number of integer variables. If the residual error between two epochs computed by triple difference phase algorithm was greater than a previously defined threshold for a specific phase observable the information of that frequency on the current and the previous epoch, is neglected and a new integer variable is created. The only purpose of this method is cycle slip determination. For each epoch and for each frequency with low residual errors, i.e. with no cycle slips, a new equation is introduced.

In terms of error analysis, the combination of both algorithms is extremely advantageous. Triple difference phase algorithm induces small errors from one epoch to the following. Nevertheless, with time, it drifts from the correct measurement, mostly because the algorithm accumulates errors from an epoch to the next. Error spectral analysis shows that, in terms of the low frequency component, this algorithm has rather high values. On the other hand, as far as the high frequency components are concerned, the values are small. In comparison, ambiguity resolution algorithm leads to higher residual errors than triple difference phase algorithm (considering only the errors induced from an epoch to the following). However, the ambiguity resolution algorithm does not present any drifts since it is an absolute method. The spectral behaviour of this algorithm is defined by small values in the low frequency component, and high values in high frequen-

cies. The error signal from the ambiguity resolution algorithm has a very small mean value, but varies more than the one from triple difference phase algorithm from epoch to epoch. The combination of these two algorithms brings together good features on high frequencies of the triple difference phase algorithm and a great performance on low frequencies of ambiguity resolution algorithm. Moreover, this combination reduces computational effort, since triple difference phase algorithm leads to lower processing effort than ambiguity resolution algorithm. Figure 5.3 sketches the description mentioned before.

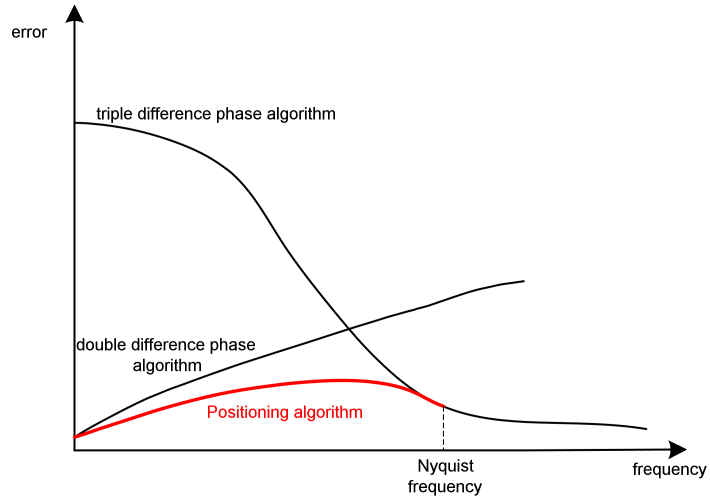

Figure 5.3 — Schematic view of the error evolution for each algorithm.

Figure 5.4 shows the rover trajectory based on this algorithm. Rover position is computed by ambiguity resolution algorithm on several epochs along the course. For each epoch, when the location is correctly computed through double difference phase combination, this algorithm will compute the rover position by triple difference phase combination, assuming that the ambiguities do not change between epochs. Ambiguity resolution algorithm is computed with a rate of 1Hz and triple difference algorithm is compute in a rate of 10Hz.

Comparing this result with the one obtained in triple difference phase algorithm, the drift on the vertical plane disappears due to the introduction of new equations that help determine the correct location of the rover. Also, the jitter due to residues in ambiguity resolution algorithm is attenuated.

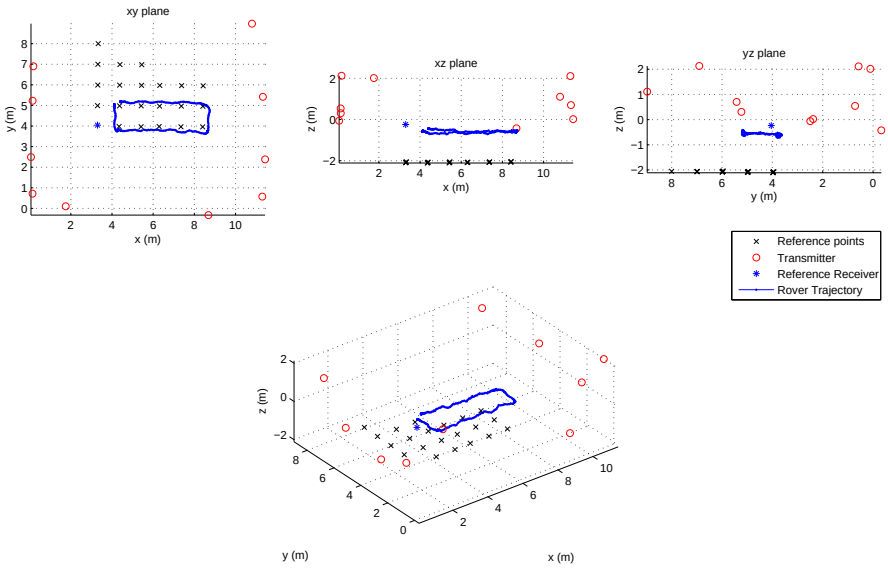

Figure 5.4 — Rover trajectory with multiple epoch algorithm.

5.4 Most Probable Location Algorithm

In order to assess the ability of ambiguity search algorithms to distinguish good from bad candidates, an algorithm that finds the most probable rover receiver position for each epoch within a search region was created. This algorithm admits different position estimates for the roving receiver and, for each one, computes the double difference phase combination of the real acquired data. This measurement is then compared to the data associated with the geometry of the transmitters and receivers in rover position. The residue of the difference between the real data and the data obtained from the positioning estimates (virtual data) lead to the probability of the roving receiver being in that precise location. This algorithm involves searching for solutions in a large set of locations. Therefore, it is highly inefficient. Its only purpose is to check good positioning of transmitters relative to rover, good choice of frequencies, and also that the measurements are correct.

Expanding 3.29 and converting the phase from metres into cycles the result

is expressed as,

$$\Delta\Delta\phi_{kl}^{ij} = -[1/\lambda^i(D_k^i - D_l^i) - 1/\lambda^j(D_k^j - D_l^j) + (f^i - f^j)\Delta t_{kl}] + N_{kl}^{ij} \quad (5.14)$$

with $(f^i - f^j)\Delta t_{kl}$ as the differential receiver clock error (in the general situation the receiver clock error cannot be the same, so this term could not be eliminated).

Ambiguities N_{kl}^{ij}, could be written as expressed in 5.15,

$$N_{kl}^{ij} = \Delta\Delta\phi_{kl}^{ij} + [1/\lambda^i(D_k^i - D_l^i) - 1/\lambda^j(D_k^j - D_l^j) - (f^i - f^j)\Delta t_{kl}] \quad (5.15)$$

The double difference phase observable of acquired data is given by,

$$\phi_{real} = \phi_{rov}^i - \phi_{ref}^i - \phi_{rov}^j + \phi_{ref}^j \quad (5.16)$$

where ϕ_{rov}^i is the phase acquired by the roving receiver of the i^{th} transmitter, ϕ_{ref}^i is the phase acquired by the reference receiver of the i^{th} transmitter, ϕ_{rov}^j is the phase acquired by the roving receiver of the j^{th} transmitter and ϕ_{ref}^j is the phase acquired by the reference receiver of the j^{th} transmitter.

The virtual data is expressed by,

$$\phi_{virtual} = -[1/\lambda^i(D_k^i - D_l^i) - 1/\lambda^j(D_k^j - D_l^j)] + (f^i - f^j)\Delta t_{kl}] \quad (5.17)$$

Therefore, the probability of the roving receiver being in that position is related to,

$$Prob = cos(2\pi(\phi_{real} - \phi_{virtual})) \quad (5.18)$$

The purpose of the cosine is to allow the matching ambiguities to get closer to integer (residues are small) [Hal02]. This expression is not exact as a probability calculation; it is rather a practical mean to estimate the likelihood of each rover position.

Chapter 6

Results and Discussion

Summary: *This chapter is devoted to the presentation and the critical analysis of the results obtained by the developed algorithms and described in chapter 5.*

The results presented in this chapter were acquired through phase signal processing with the implemented algorithms, described previously. As mentioned before, the experimental setup implemented had ten transmitters spread around the room in different directions, each of them transmitting a single frequency, to assure an efficient and accurate tracking of the roving receiver.

6.1 Positioning Algorithm

Several experiences were conducted by moving the rover around the room. Figures 6.1 and 6.2 illustrate a schematic view on the horizontal plane of a few routes performed by the rover. All motions were executed by a person holding the microphone (receiver). The height did not exceed 30cm below the reference receiver, which was placed 2m above the floor. The motion speed was almost constant during the experience. The human gait, as a periodic motion, could induce disturbances on the position of the rover related with the schematic view shown in figures 6.1 and 6.2.

A few points were marked as a visual reference to help rover trajectory perception. These points were physical marks on the room floor. The trajectory was performed around those points. The origin was marked as the most convenient and visible point on the photos used for stereoscopic image processing. This position, as all the points marked on the schematic view, were also determined by methods of stereoscopic image comparison. All the points and the photos available lead to this layout. The transmitters were considered as a point source because its dimension, when compared to the dimension of the room and the magnitude of the used wavelengths, is negligible.

The final positioning algorithm determines the location of the rover by ambiguity resolution, retrieving information from several epochs and keeping phase measurements coherent through triple difference phase combinations. This algorithm is able to detect the most probable position of the rover and correct

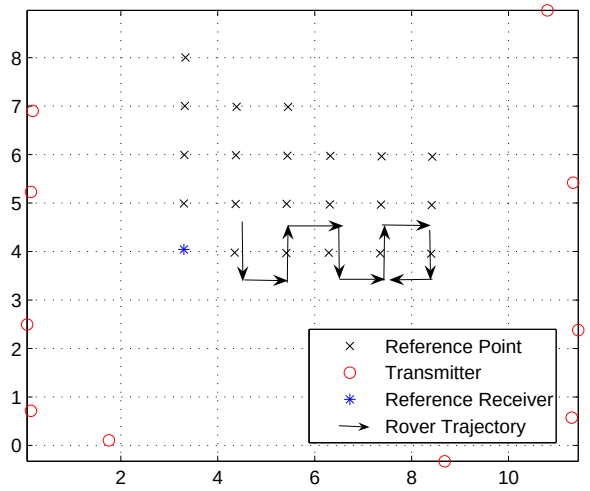

Figure 6.1 — Schematic view of rover motion.

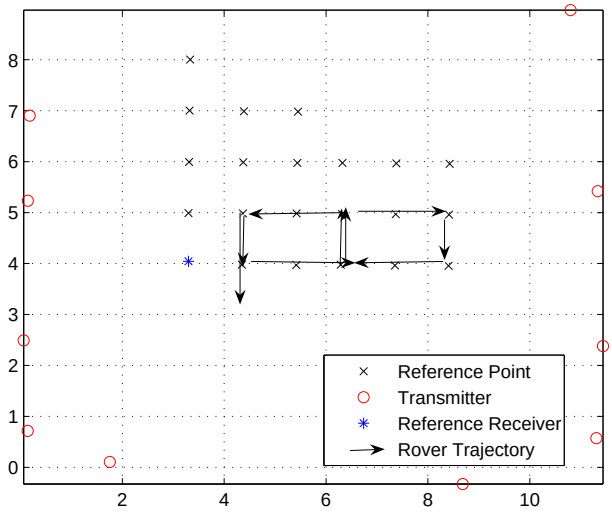

Figure 6.2 — Schematic view of rover motion.

triple difference phase algorithm whenever cycle slips occur. The acquired and processed signal leads to the trajectories described in figures 6.3 and 6.4.

These results describe correctly the executed motion by the rover, corre-

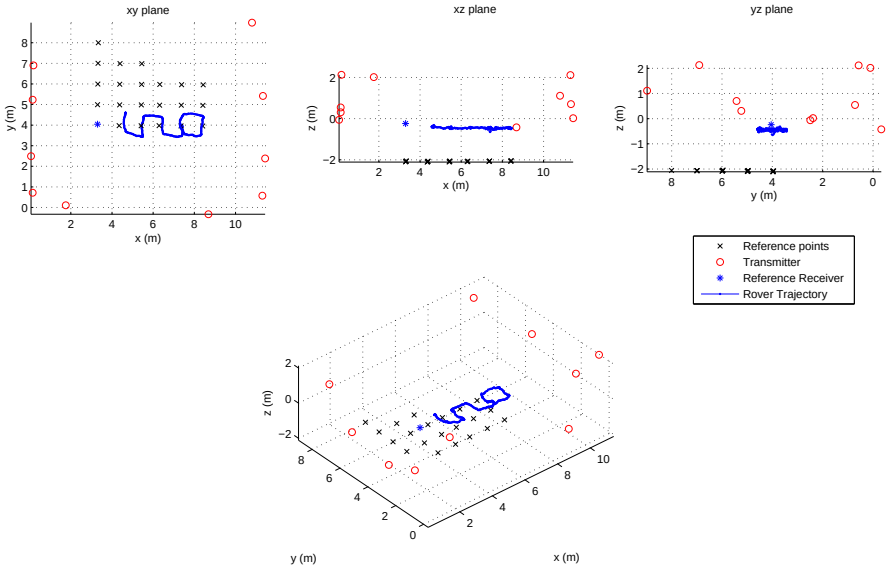

Figure 6.3 — Acquired and processed data.

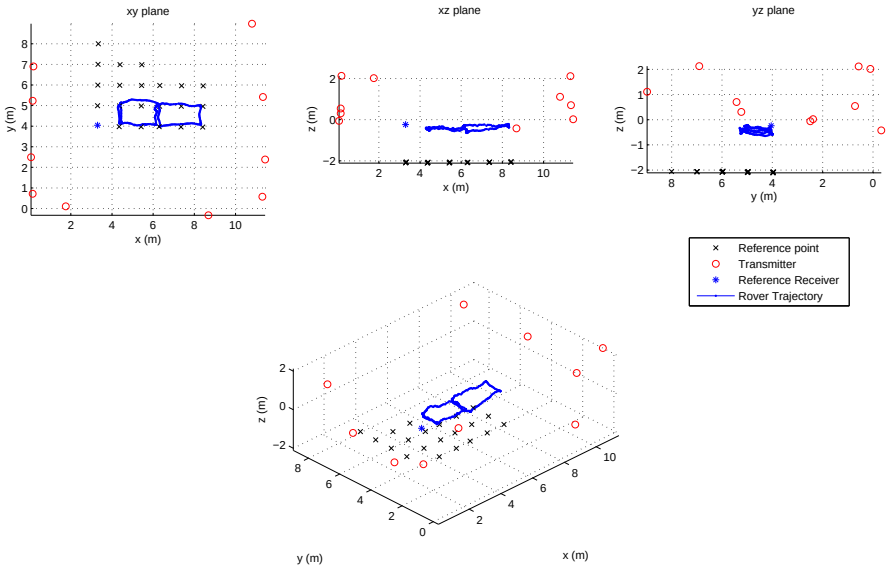

Figure 6.4 — Acquired and processed data.

sponding to figures 6.1 and 6.2. Possible cycle slips during phase measurements were detected and corrected. Seven of ten available frequencies were used, which were the ones with a lower cycle slip occurrence. Besides the fact that the experiments, shown in figures 6.3 and 6.4, do not have significantly changes on height, the developed algorithms provide also to the correct navigation solutions in the

presence of height variations, as can be seen in figure 6.5. This figure illustrates a quarter of a circle executed along the yz-plane. The results achieved by the positioning algorithm lead to the correct course, with an accuracy equal to others experiences shown before. This accuracy is studied later through residues analysis.

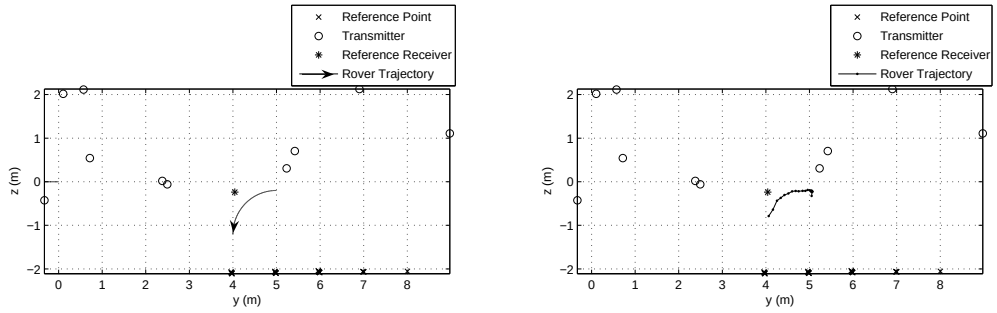

Figure 6.5 — Acquired and processed data.

6.1.1 Accuracy Analysis

Residue analysis was conducted so as to assess result accuracy. As illustrated in figure 6.6, where residues relating to the movement described in figure 6.1 are shown, the errors are consistently below a quarter of the cycle, i.e. in 25% of the wavelength of each signal. In metres, figure 6.6 is expressed by 6.7. Through observation, it has been assessed that residues represent an error with a maximum value of 7cm in the lowest frequency and a minimum value of 7mm in the highest frequency.

Figure 6.8 shows the tracks performed by the roving receiver in detail where the positions were computed for a few epochs by double difference phase combination, as well as the evolution by triple difference phase combination from each position that is determined with ambiguity resolution algorithm. In figure 6.8 the errors induced by phase measurements are small (even though they exist). These errors can be induced by echoes and/or by uncertainty of the transmitter

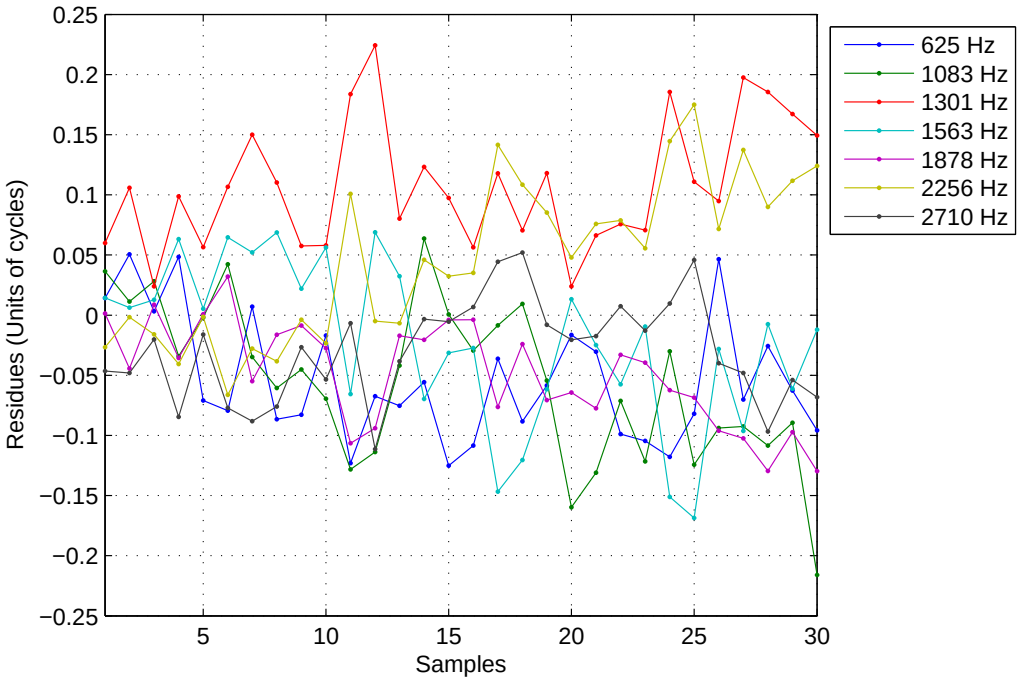

Figure 6.6 — Residues in unit of cycles relative to the course presented in 6.1.

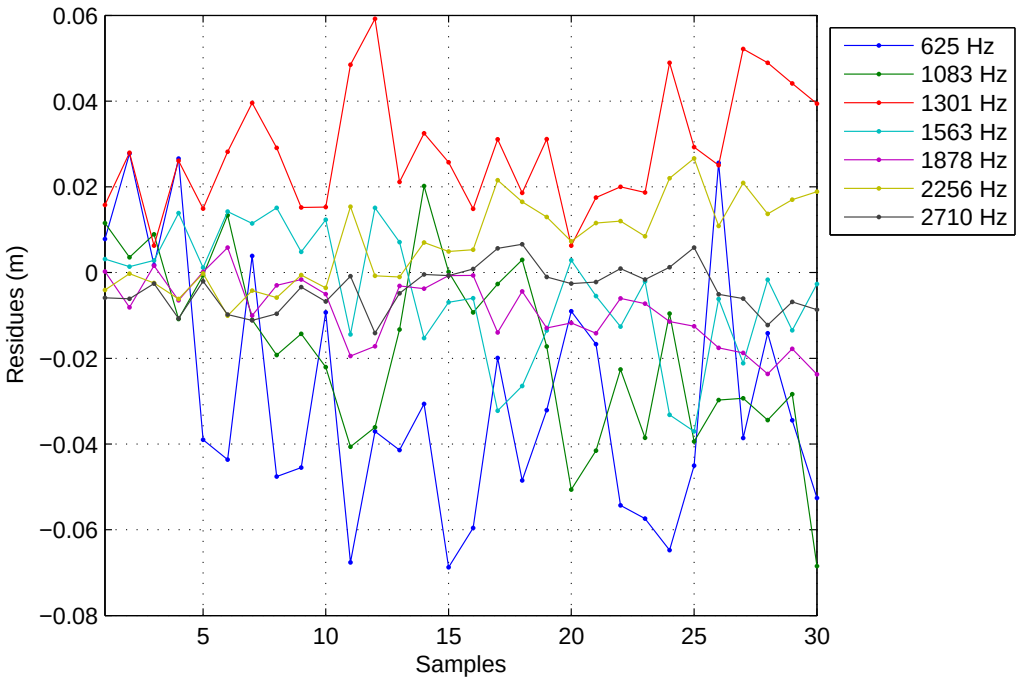

Figure 6.7 — Residues in metres relative to the course presented in 6.1.

positions. As far as the vertical position is concerned, the differences found are also caused by gait motion, which contributes with an inconstant level.

Echoes are reflections of the transmitted signal on the objects or on the walls of the room. They generate new signals with the same frequency of those used in the system, but with a power level lower than the originals. The echoes are equivalent to virtual transmitters with the same frequencies that are used on the experiment so, in fact, this new signal proceeds from different directions of the original signals. The influence of two signals having the same frequency and proceeding from different locations destroys the spherical pattern of the origin signal, which induces disturbances on the phase information. The influence of echoes on determining the correct rover location is, mostly, related to the reflected power level. If the reflections have a very small power level, the influence on the original signal is almost negligible. However, this work proofs that reflections in acoustic waves have almost the same order of magnitude of the original signal. In this sense, the presence of echoes is considered as a major cause of error in terms of rover location. So, the use of an anechoic chamber in this work proved very valuable as this infrastructure succeeds in mitigating the effect of echoes.

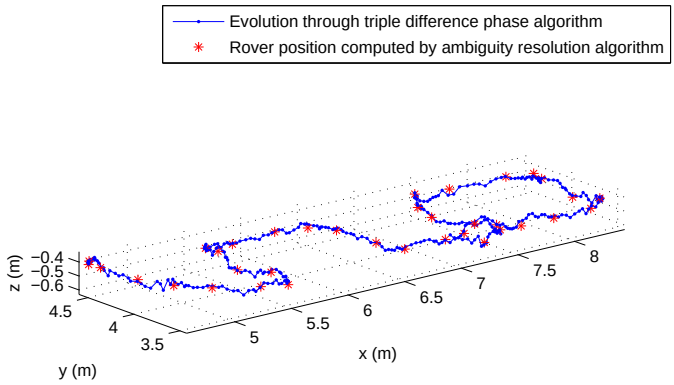

Figure 6.8 — Rover evolution by triple difference phase combination and some position determined through double difference phase combination.

6.2 Most Probable Location Algorithm

To check if the position in a specific time frame was correct, another algorithm, also explained in chapter 5, was implemented. This algorithm is based on double difference phase combination and determines the probability of the rover being in a previously defined search area. This algorithm is a verification method, and tests the feasible solutions discrimination ability of ambiguity resolution method to determine the rover location.

Figure 6.9 presents the probability of the rover being in that position considering only the information of one epoch, in a given search area. The highest probability regions are represented in red and the lowest probability regions are in blue. The search area is 2m×1.5m. One of the highest probability regions corresponds to the point estimated by the photographic survey of several photos taken to the layout, which is marked in figure 6.9 as a black dot.

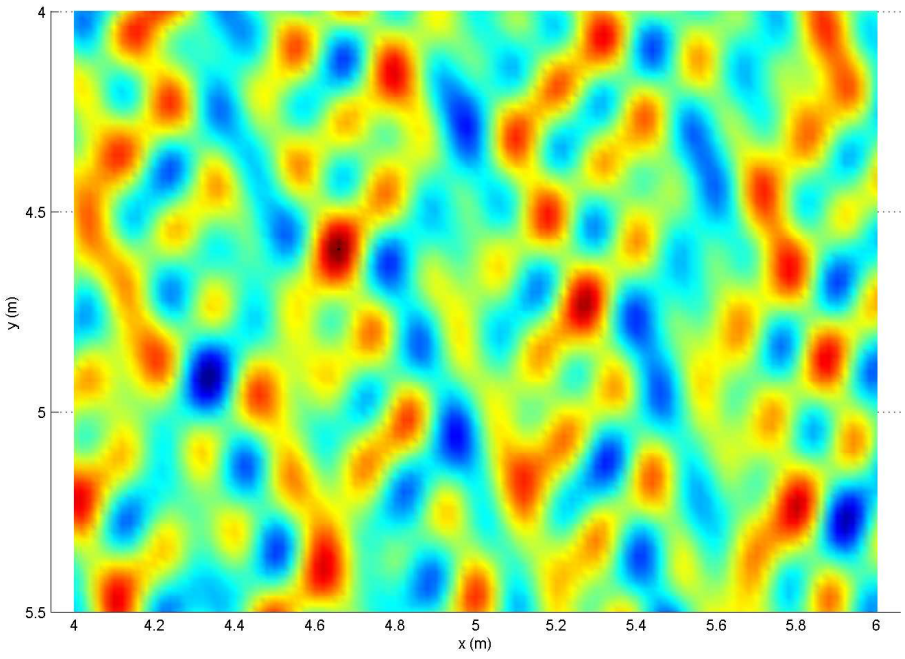

Figure 6.9 — Probability of the rover location in a specific search area considering the information of one epoch.

The rover location, which is determined by the positioning algorithm, corresponds to one of the highest probability regions. However, other regions with high probability could also be possible. The highest probability solutions are consistent with the solution with lower residues. If the probability was determined with the information of more than one epoch, the coherence of the system would lead only to one available solution.

Figure 6.10 shows the same algorithm with the same search area as figure 6.9, but considering data of a set of several different epochs. The evolution with triple difference combination blended with the coordinates of the initial position of the rover for several epochs, leads to enhancement of the peak corresponding to the correct solution relative to other peaks, due to the coherence of phase measurements. The presence of motion is very important when it is taking into account the verification method considering several epochs. Otherwise, the coherence pattern obtained would be similar to the one illustrated on figure 6.9, once that triple difference evolution without motion would conduce exactly to the same location results for all epochs. Notice that there is only one region of high probability, which corresponds exactly to the position determined by ambiguity resolution algorithm.

The information of more than one epoch increases the number of equations of the system and contributes to a more accurate result. The region of higher probability is very restricted and converges to the correct solution, even when the search area is wider than the search region shown here. As mentioned on section 1.4, the feasible solutions for rover positioning are the highest probability regions. These highest probability regions correspond to the intersection of wavefronts of n transmitters (in this case seven), as similarly illustrated in figure 1.2 which is a two-dimensional case with only three transmitters.

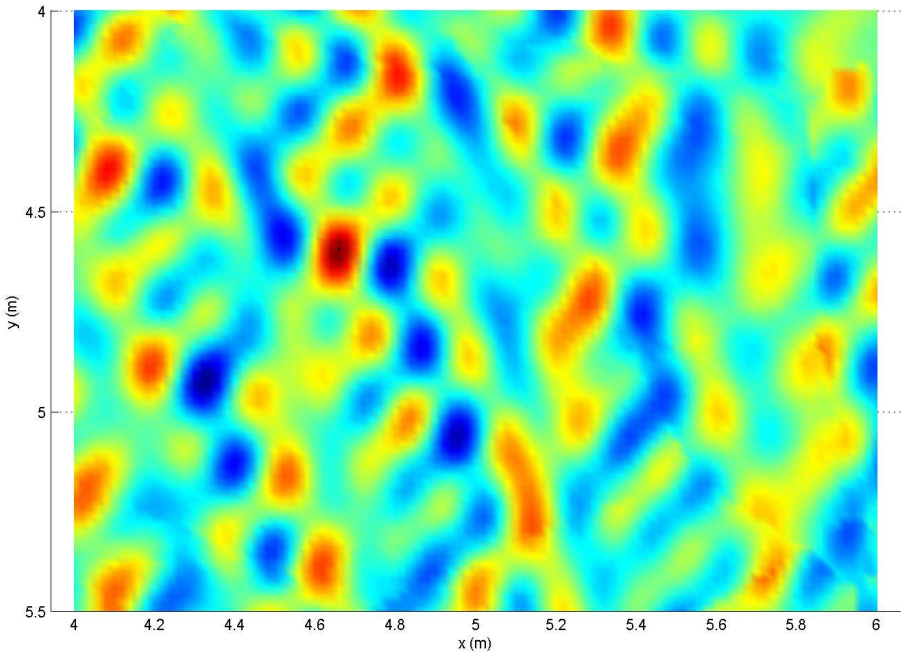

Figure 6.10 — Probability of the rover location in a specific search area considering the information of several epochs.

Chapter 7

Conclusions and further work

Summary: *This chapter presents the conclusions of the work and several subjects that are to be addressed as future research.*

The results obtained until now lead to several important conclusions that allow the validation of the initial concept: location detection by sound wave phases processing.

7.1 Conclusions

The direct conclusion from this work is that instantaneous positioning is possible using phase processing of acoustic signals.

The frequencies used in this system had to be taken into account in all phase observations. The frequencies were chosen according to a distribution that avoids beat frequencies of two single frequency signals around a third frequency in the admitted band. Also, the used wavelengths need to have the same magnitude as if they were to be used in RF applications.

The presence of echoes introduces phase shifts following complex patterns on the acquired signal, since this reflection corresponds to a signal from a virtual transmitter which destroys the spherical pattern of the original signal. The acoustic reflections have almost the same order of magnitude as the original signal so the interference is notorious. The use of an anechoic chamber became one of the most important requirements of this work.

Phase measurements can be computed from processing the acquired data. This pre-processing step converts the acquired data collected into instantaneous phase and amplitude estimates based on three cascaded low-pass finite impulse response (FIR) filters. The use of FIRs filters was compared with the FFT method and proved to be an efficient solution to determine phase information, from raw data, in a real-time processing. Besides this method had a higher computational effort than the FFT method, in this work the use of FIRs filters was less prone to implementation errors.

Observation equations were developed and represent a generalization of positioning observables for single frequency signals. Combinations between re-

ceivers and transmitters allow the elimination of transmitter and receiver clock errors. However, this method introduces an integer term (single difference ambiguity) which is not present in others positioning systems that use modulated signals that convey timing information.

The positioning algorithm consists on determining the exact position by double difference phase combination processing. This processing takes the information of several epochs into account which contributes to more accurate results. The information of several epochs is important in spite of increasing the number of equations of the system. It contributes also to a more accurate result. The coherent behaviour of the signal lead typically to only one most probable solution. To reduce the processing effort, the evolution is determined by triple difference phase combination, assuming ambiguities are constant during the period of time from one correct position computed by double difference phase combination to the next one. Cycle slips are detected and eliminated through residue analysis.

The n-dimensional integer optimization problem was successfully solved through ambiguity resolution algorithm based on double differences combination, which is expressed as a weighted least squares minimization problem with real and integer variables. The LLL algorithm was an efficient method to determine the base vectors as short as possible and reasonably orthogonal. The rover trajectory was determined by triple difference phase combination blended with ambiguity resolution. The computed trajectory corresponds to the course made by the rover. The residues obtained for ambiguity resolution results, for each experiment, lead to an accurate solution with an uncertainty below 7cm, statistically in the order of 3cm.

To check the reliability of the positioning method, another algorithm was developed to describe the highest probability regions for a search area previously defined. The results are consistent with the real rover positioning determined by photographic survey of the layout. With this algorithm a pattern of probabilities for a predefined region is obtained. The highest probability regions are equivalent

to the feasible solutions of this n-dimensional integer optimization problem.

7.2 Future Research

This work tries to prove that positioning with phase processing of signals, with no additional information, is possible. The similarities between this work and others applications, such as RF based systems, are the following:

On an RF based application several signals of opportunity on which only the carrier signal is used, are necessary. For this system a set of reference receivers would also be necessary in order to determine phases relating to a known position, as well as waves propagation directions.

The wavelengths that should be used in this kind of application correspond to signals in VHF and UHF (possibly microwaves). The use of TV and radio broadcast stations are an efficient way to achieve radiolocation with centimetric accuracy. These opportunity signals have to be plane waves above the order of magnitude of the distance between receivers.

To roughly synchronize the data acquired, a pseudo-random binary sequence code (PRBS) could be placed in one of the transmitting channels (which would not be an opportunity signal). This PRBS code would be responsible for transmitting information to the rover. The PRBS code could also be useful to provide other information such as:

- transmitters location/direction;

- reference receiving station location;

- reference receiving station signal (phases);

- other useful information.

Instead of the PRBS code, this information could be transmitted through

Wi-Fi. This alternative way to transmit information would lead to worse results on time adjusting.

The parallelism between this work and a future application in RF signals became obvious, since the developed algorithms could be applied also with phases processing of RF signals.

Besides positioning with phase processing of signals could be applied on RF signals, this approach has direct applications in underwater location systems. As RF signals do not penetrate well on water (due to the higher attenuation induced by this fluid) the results of this work can be useful in such specific navigation environments.

Bibliography

[AF99] Marcelo Alonso and Edward Finn. *Física*. Addison Wesley Longman Ltd, January 1999.

[AWWJ03] M. Abdel-Hafez, W. Williamson, J. Wolfe, and Speyer J. A high-integrity and efficient gps integer ambiguity resolution method. *Journal of the Institute of Navigation Winter 2003/2004*, 50(4):295–310, 2003.

[BP00] P. Bahl and V. N. Padmanabhan. Radar:an in-building rf-based user location and tracking system. In *Proceedings IEEE INFOCOM2000, Vol. 2*, March 2000.

[Cyg04] D. Cygansky. Performance of a precision indoor positioning system using a multi-carrier approach. In *Proceedings of the National Technical Meeting, Institute of Navigation 2004, pp 175-180*, January 2004.

[DA01] F. Diggelen and C. Abraham. Indoor gps technology. In *CTIA Wireless-Agenda*, May 2001.

[DR01] G. M. Djuknic and R. E. Richton. Geolocation and assisted gps. *IEEE Computer*, 34(2):123–125, 2001.

[dTT96] P. de Jonge, C. Tibernius, and P. Teunissen. Computational aspects of the lambda method for gps ambiguity resolution. In *Proceedings of ION GPS-96 9th International Technical Meeting of the Satellite*

Division of the Institute of Navigation, pp. 935-944, 17-20 September 1996.

[Hab99] H. Habrich. *Geodetic Applications of the Global Navigation Satellite System (GLONASS) and of GLONASS/GPS Combinations*. PhD thesis, Univertität Bern, November 1999.

[Hal02] T. Hall. *Radiolocation Using AM Broadcast Signals*. PhD thesis, Massachusets Institute of Technology, September 2002.

[HB98] A Hassibi and S Boyd. Integer parameter estimation in linear models with applications to gps. *IEEE Transactions on Signal Processing*, 46(11):2938–52, 1998.

[HBW02] J. Hightower, G. Borriello, and R. Want. Spoton: An indoor 3d location sensing technology based on rf signal strength. In *Technical Report UW CSE 2000-02-02*, February 2002.

[HHS+99] A. Harter, A. Hopper, P. Steggles, A. Ward, and P. Webster. The anatomy of a context-aware application. In *Proceedings of the 5th Annual ACM/IEEE International Conference on Mobile Computing and Networking (MOBICOM 99)*, August 1999.

[HMK98] G. Havas, B. Majewski, and Matthews K. Extended gcd and hermite normal form algorithms via lattice reduction. *Experimental Mathematics*, 7(2):125–136, 1998.

[KFCS82] Lawrence Kinsler, Austin Frey, Alan Coppens, and James Sanders. *Fundamentals of Acoustics*. Addison Wesley Longman Ltd, January 1982.

[LCL00] Paul Lorrain, Dale Corson, and François Lorrain. *Campos e Ondas Electromagnéticas*. Fundação Calouste Gulbenkian, March 2000.

[PCB99] N. B. Priyantha, A. Chakraborty, and Balakrishnan. The cricket location-support system. In *Proceedings ACM/IEEE International Conference on Mobile Computing and Networking (MOBICOM 00), Boston*, August 1999.

[Ros88] Mario Rossi. *Acoustics and Electroacoustics*. Artech House, Inc, 1988.

[SL04] M. Shah and Y. C. Lai. Performance of integer parameter estimation algorithm for gps signals in noisy environment. In *ION GNSS International Tecnical Meeting of the Satellite Division: Proceedings of the ION Meeting, pp. 166-174*, 21-24 September 2004.

[WHFG92] R. Want, A. Hopper, V. Falcão, and J. Gibbons. The active badge location system. *ACM Transactions on Information Systems*, 40(1):91–102, 1992.